THE UNIVERSITY OF ALBERTA

# THE PRECAMBRIAN ROCKS OF THE OLD FORT POINT FORMATION - JASPER, ALBERTA

A THESIS

SUBMITTED TO THE FACULTY OF GRADUATE STUDIES

IN PARTIAL FULFILMENT OF THE REQUIREMENTS FOR THE DEGREE

OF MASTER OF SCIENCE

DEPARTMENT OF GEOLOGY

by

CALVIN RALPH EVANS, B.Sc.

EDMONTON, ALBERTA

April, 1961

## ABSTRACT

The Old Fort Point formation of the Jasper anticlinorium comprises some 1200 feet of argillite, siltstone, limestone, and limestone-breccia, probably Precambrian in age. The sequence, divided into four members, probably records the westward migration of an ancient delta. Member A, the oldest, displays some 350 feet of argillaceous bottomset beds, while the overlying 500 feet of member B strata represent the foreset beds, characterized by numerous lenses of intraformational limestone-breccia. A break in the orderly sequence of events is recorded by the several hundred feet of homogeneous argillite of member C. However the 150 feet of silty argillite and siltstone of member D, overlain conformably by sandstone and quartz pebble conglomerate of the Miette formation probably represents the final phase of the transition from fairly deep water, to very shallow water deposition.

These rocks were tightly folded into a series of overturned anticlines and synclines, comprising the Jasper anticlinorium, and elevated to their present structural position by movement along the Pyramid thrust-fault during the Laramide orogeny. Flow-cleavage, fracture-cleavage, and cleavage-boudinage are well developed and excellently exposed. Nine joint-sets record the complicated nature of local stress-systems throughout the tectonic history of the anticlinorium.

Observed mineral assemblages are typical of the quartz-albite-muscovite-chlorite subfacies of the greenschist facies. These minerals appear to have been in stable equilibrium with calcite, indicating very low grade regional metamorphism in the presence of a relatively high carbon dioxide partial pressure.

# ACKNOWLEDGMENTS

The writer wishes to extend his sincere gratitude to Dr. H.A.K. Charlesworth for his able direction both in the field and in preparation and writing of this thesis. To Dr. S.J. Nelson, for his many excellent suggestions regarding the stratigraphic portion of the study, the writer is also indebted. Dr. H. Baadsgaard and Dr. F.A. Campbell made it possible to include the sections on potassium-argon age determination, and X-ray analysis, respectively. For critically reading the manuscript, the writer extends his sincere thanks to Dr. K.A.W. Crook, of the Department of Geology, Australian National University, as well as to the members of the departments of Geology and of Physics, University of Alberta.

Financial assistance from a Graduate Research Fellowship presented by Imperial Oil is gratefully acknowledged. Grants from the Shell Oil Company of Canada, Ltd., and from the Department of Geology defrayed field expenses and preparation costs. This research is part of a large project on the Precambrian geology of the Jasper region which is being supported by the Research Council of Alberta.

TABLE OF CONTENTS

# LIST OF TABLES, FIGURES AND PLATES

# INTRODUCTION

The thesis subject is a study of the stratigraphy, structure, and metamorphism of the oldest known rocks in the vicinity of Jasper, Alberta. The map-area lies in the main ranges of the Canadian Rocky Mountains at latitude 52° 52' and longitude 118° 05'. The Pyramid thrust-fault outcrops some 3 miles to the northeast, marking the boundary between the Precambrian and Lower Palaeozoic strata of the main ranges and the predominantly Upper Palaeozoic beds of the eastern ranges.

The Old Fort Point formation (Charlesworth and Remington, 1960, p. 13) was mapped for a distance of 7 1/2 miles in the core of an anticlinorium which passes through the town of Jasper, the boundary of the map-area being the contact of this formation with the conformably overlying Miette formation (Figure 1). The area is 1 1/2 miles wide where the Athabasca River cuts through the anticlinorium, but narrows to the northwest and southeast due to the doubly plunging nature of the structure. The southeastern extremity of these rocks is as yet unmapped.

## STRATIGRAPHY

Introduction. The argillaceous and calcareous strata of the Precambrian Old Fort Point formation, the oldest exposed in the Jasper anticlinorium, differ greatly from the overlying, predominantly arenaceous Miette formation. The former is divided into four easily distinguished members with a maximum composite thickness of up to 1200 feet. In descending order these are:

Member D 150 feet of silty green and bluish green argillites which become more arenaceous near the contact with the conformably overlying Miette formation.

Member C up to 250 feet of dark bluish grey argillite, weathering dark rusty brown, with a quartzose limestone-breccia near the top in the southwestern part of the anticlinorium.

Member B 500 feet of greenish grey, laminated argillites with interbedded thin siltstones, limestones, and lenticular limestone-breccias.

Member A 350 feet of dark bluish grey argillite with interbedded siltstones near the top.

Member A. The type-section of member A (Figure 1) is on the northeast bank of the Athabasca River some 900 feet southeast of the bridge (Figure 2). The upper interbedded siltstones and argillites are exposed in the core of the anticlinorium for a short distance on either side of the river

valley, but the lower argillites, whose base is not exposed, outcrop only at the type locality. Within the map-area, member A is composed of the following rock types:

Argillite. The basal beds are homogeneous, dark bluish grey, poorly laminated, and well cleaved argillites composed chiefly of chlorite, muscovite, and quartz. Half-inch greyish orange bands of silty, iron-stained argillite occur at intervals of several feet throughout the lower part of the member. Towards the top, the argillite becomes grey, silty, and poorly cleaved.

Siltstone. Siltstone is largely confined to the upper part of the member, with beds becoming thicker and more closely spaced towards the top, where siltstones 6 inches to 3 feet thick are separated by 1- to 6-inch bands of argillite. They are generally dark bluish grey weathering brown, and consist of angular quartz and albite grains together with books of chlorite and muscovite in a matrix of calcite, limonite, and fine-grained muscovite and chlorite.

Member B. The type-section of member B (Figures 1 and 2) is along the northwestern slopes of Old Fort Point. Besides being the thickest and best exposed member of the Old Fort Point formation, it is the most distinctive, being characterized by bedded limestones and limestone-breccias. Member B is thickest in the northeastern part of the anticlinorium, and thins to the southwest. It consists of the following rock-types:

FIGURE 1. Composite type-section of the Old Fort Point formation. The section on the right has been corrected for tectonic variation in thickness.


MIETTE FORMATION
OLD FORT POINT FORMATION
MEMBER D
150 feet
MEMBER C
250 feet
MEMBER B
480 feet
Breccia
MEMBER A
335 feet
Meosured Section
1215 feet
MIETTE
MEMBER D
150 feet
MEMBER C
305 feet
MEMBER B
455 feet
Breccia
MEMBER A
380 feet
Corrected Section
1290 feet
INTERBEDDED SANDSTONE AND SILTY ARGILLITE
NODULAR ZONE
INTERBEDDED SILTSTONE AND SILTY ARGILLITE
BLUE IRON-STAINED ARGILLITE
ARGILLITE WITH LENS OF LIMESTONE BRECCIA
INTERBEDDED ARGILLITE AND SILTSTONE

Figure 1

FIGURE 2. Map showing the location of type-sections, stratigraphic sections, structural sections and sub-areas A to E.

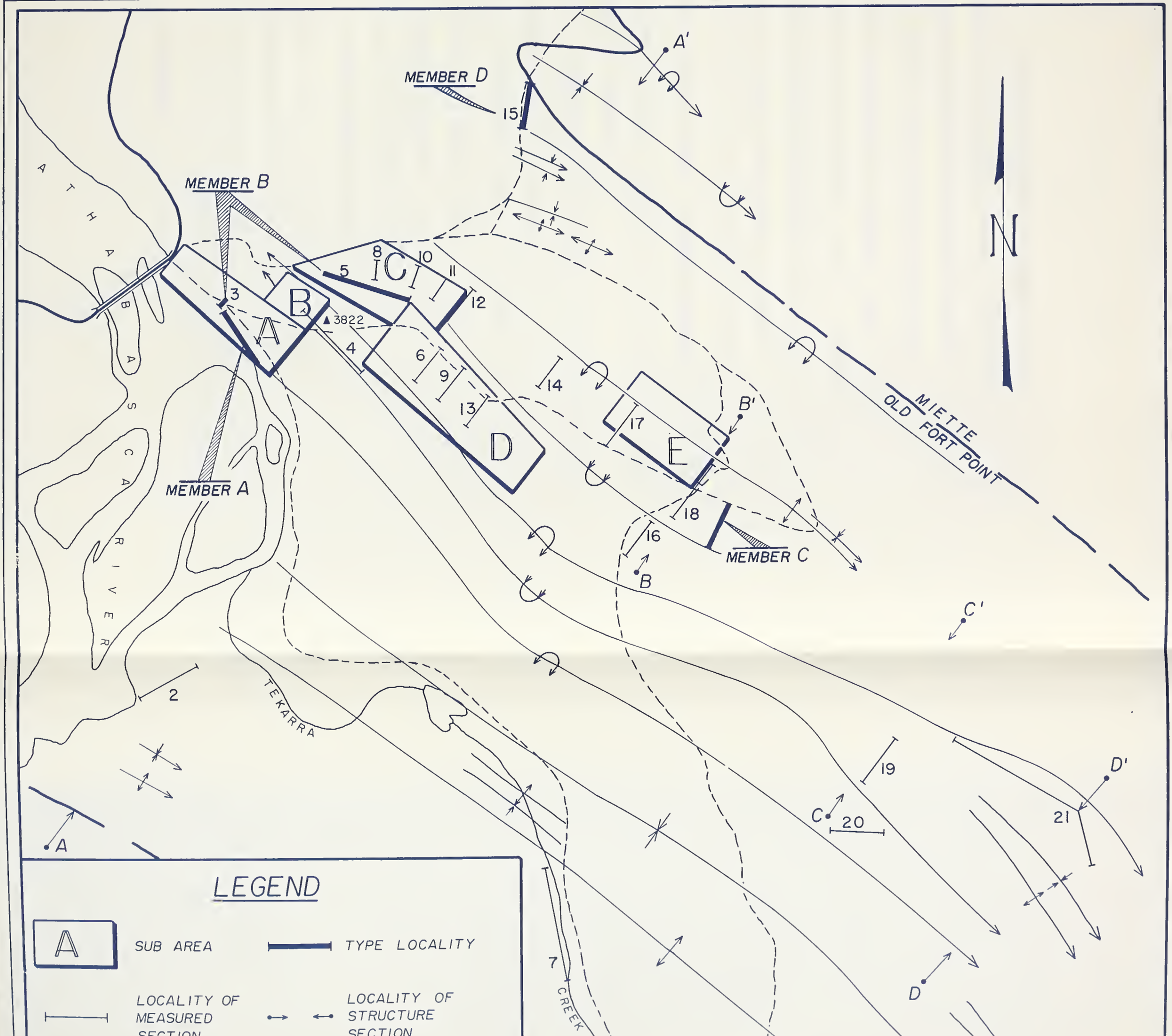
A'
MEMBER D
15
MEMBER B
A T H A B A S C A
RIVER
3
B
A
5
8
IC I
10
11
12
▲3822
4
6
9
13
D
14
17
E
B'
MIETTE
OLD FORT POINT
N
18
16
MEMBER C
B
C'
MEMBER A
2
TEKARRA
19
C
20
D'
21
D
A
7
CREEK
LEGEND
A
SUB AREA
TYPE LOCALITY
LOCALITY OF MEASURED SECTION
LOCALITY OF STRUCTURE SECTION

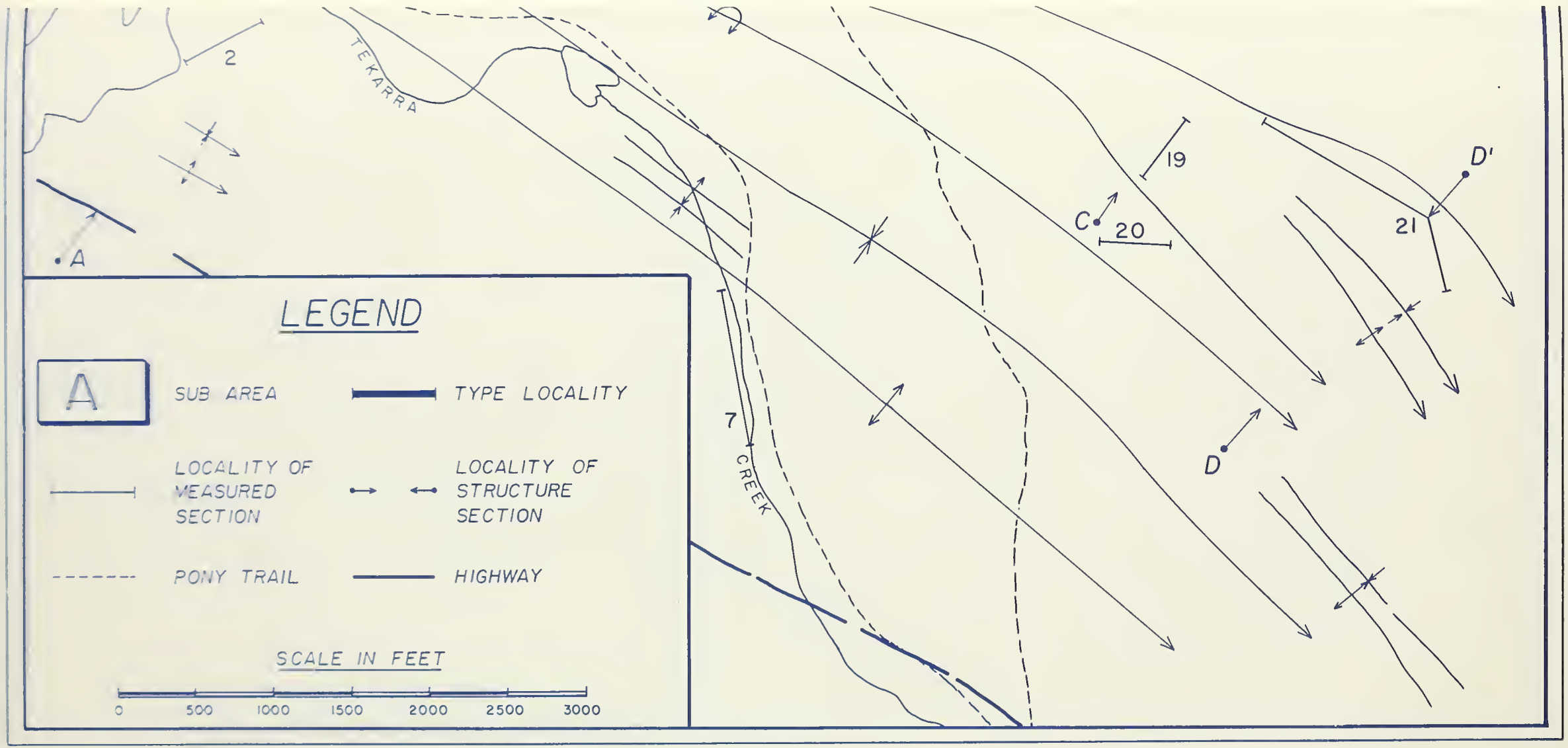
2
TEKARRA
A
19
C
20
21
D'
D
7
CREEK
LEGEND
A
SUB AREA
TYPE LOCALITY
LOCALITY OF MEASURED SECTION
LOCALITY OF STRUCTURE SECTION
PONY TRAIL
HIGHWAY
SCALE IN FEET
0
500
1000
1500
2000
2500
3000

FIGURE 2

Argillite. Seventy to ninety per cent of member B is composed of greenish grey argillites with numerous brown silty laminae. Very fine-grained chlorite and muscovite particles parallel the cleavage, but books of chlorite with interlayered muscovite, 0.1 to 0.2 millimetres in diameter, cross-cutting cleavage, comprise from 5 to 10 per cent of the rock. Pleochroism in both the fine- and the coarse-grained chlorites decreases progressively from bottom to top, a feature common to the chlorites of the siltstones and breccias of member B. Other components are quartz and albite with minute crystals of siderite. The argillite is calcareous near breccia lenses. In the southern and western parts of the map-area, a purple, highly calcareous, silty argillite is present in the upper half of member B.

Limestone. About 60 feet of thin-bedded limestone overlies the purple argillite on the east bank of the Athabasca River in the southern part of the area. Both the individual limestone beds and the interbedded, calcareous argillite range in thickness from 1/2 inch to 3 inches. The argillite undergoes a colour change from purple at the base to green at the top, a transition which is reflected by the limestone which is pinkish grey at the base and grey at the top. While bedding is undisturbed in the lower part, the upper 20 feet shows incipient brecciation. Cryptocrystalline calcite with minute crystals of siderite makes up about 80 per cent of the limestone, the remainder consisting mainly of small grains, less than 0.15 millimetres in diameter, of albite with chlorite, quartz and muscovite.

Limestone-Breccia. Up to 20 per cent of member B is composed of intraformational limestone-breccia. The ridge-forming breccia underlying the summit of Old Fort Point (3822 feet) is the thickest and most widespread of the numerous lenses characteristic of member B. Nearly 100 feet thick at the summit, it thins rapidly to the southeast and pinches out within a quarter of a mile. The outcrops immediately west of Jasper, and on the ridge north of Mina Lake are near the base of member B, and probably belong to this unit, indicating that it extends several miles to the northwest. Although lenses can thin very rapidly, they usually persist laterally for a distance of 100 to 200 times their maximum thickness (Figure 3). Phenoclasts of cryptocrystalline limestone, similar in every respect to that described above, comprise 30 to 60 per cent of the rock. They range in size from a fraction of an inch to several feet in the longest direction, but are never more than 3 inches thick. Their orientation is highly variable, and in general there is no preferred plane (Plate I a). However on the anticlinal crest of sub-area E (Figure 2) there is a remarkable alinement along the expected cleavage planes even though the matrix of the breccia is not cleaved, while in the gentle southeast limb of the same anticline, phenoclasts are subparallel to bedding (Plate I b). Although the pale grey phenoclasts of the upper lenses of member B are smaller, reaching a maximum dimension of only 10 inches, they appear to make up a higher percentage of the rock.

FIGURE 3. Fence diagram of the Old Fort Point formation showing the probable stratigraphy of the area before deformation. Sections have been corrected for tectonic variation in thickness, and placed in their appropriate positions with the beds unfolded. The cairn, located near the north end of the bridge at Old Fort Point, serves as a reference point.

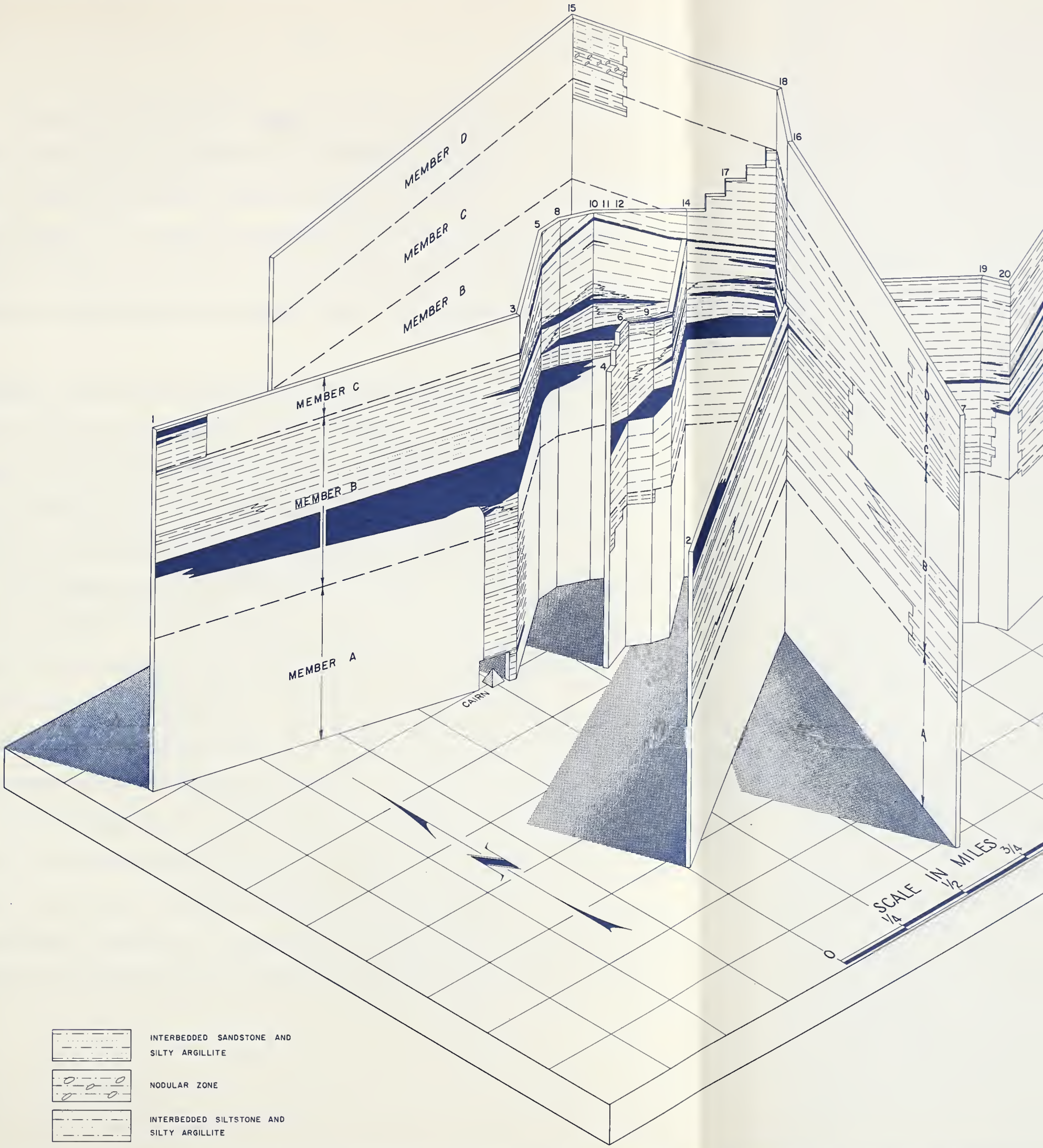
MEMBER D
MEMBER C
MEMBER B
MEMBER C
MEMBER B
MEMBER A
CAIRN
1
2
3
4
5
6
7
8
9
10 11 12
14
15
16
17
18
19
20
A
B
C
D
SCALE IN MILES
0
1/4
1/2
3/4
INTERBEDDED SANDSTONE AND SILTY ARGILLITE
NODULAR ZONE
INTERBEDDED SILTSTONE AND SILTY ARGILLITE

Figure 3

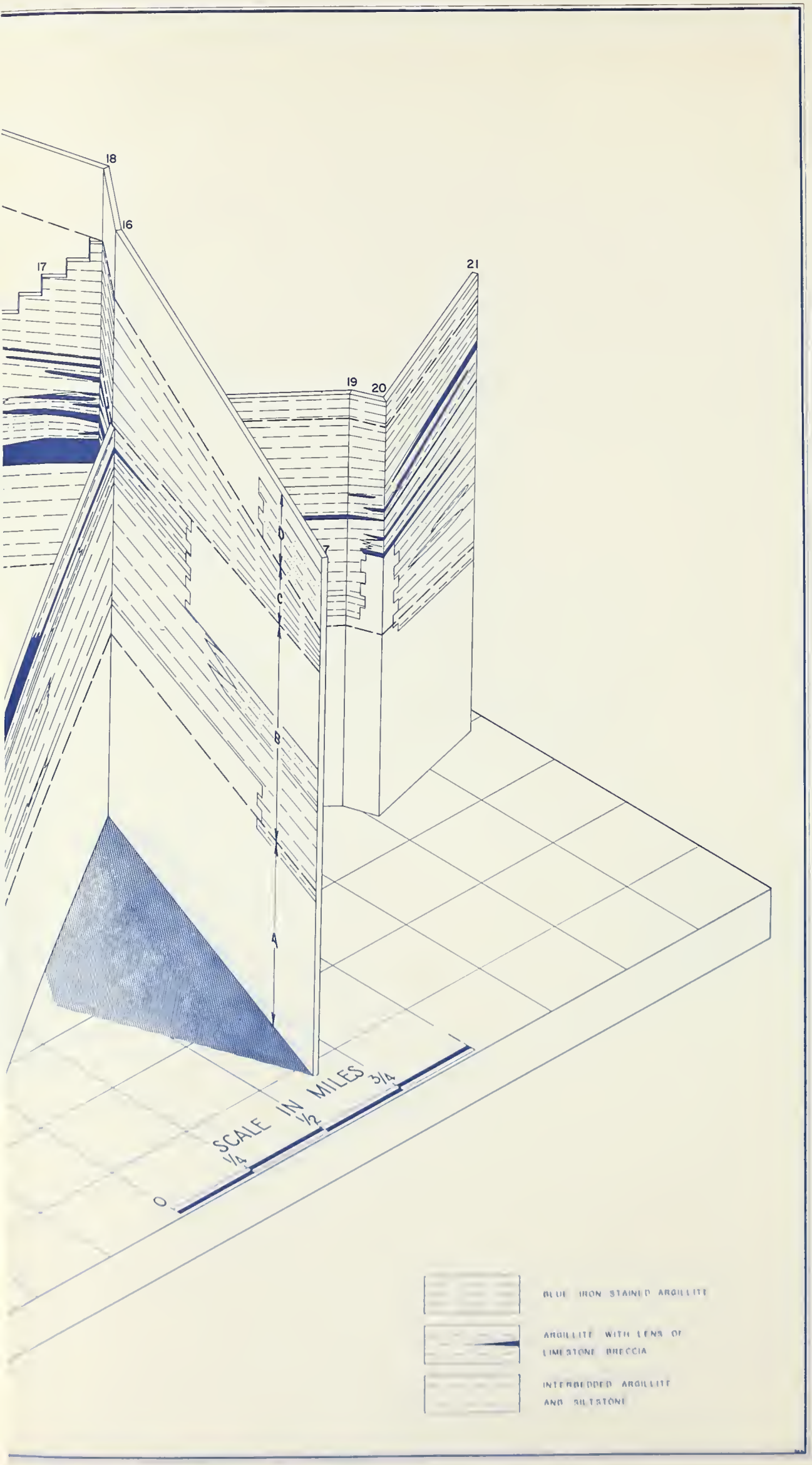
18
16
17
21
19
20
D
C
B
A
SCALE IN MILES
0
1/4
1/2
3/4
BLUE IRON STAINED ARGILLITE
ARGILLITE WITH LENS OF LIMESTONE BRECCIA
INTERBEDDED ARGILLITE AND SILTSTONE

The matrix of the lower breccia consists of silt-sized quartz, albite, and books of chlorite with interleaved muscovite, in a groundmass of cryptocrystalline calcite, chlorite, muscovite, and siderite. There appears to be less fine-grained material in the matrix of the upper breccias, and the calcite is crystalline and twinned, in contrast with the cryptocrystalline material lower in the member.

Siltstone. The maximum thickness of the siltstone lenses which comprise some 10 per cent of member B, ranges between 1 inch and 3 feet in a logarithmic normal distribution (Figure 4) common to many sedimentation units (Pettijohn, 1957, p. 160). Scour, slump, and pinch-and-swell structures as well as cross stratification are common (Plate I c, d, and e). There appears to be a progressive increase in the proportion of the granular fraction of the siltstones, increasing from 50 per cent of the rock in the lower part of the member to 90 per cent in the upper part. This fraction consists of well-sorted quartz and albite grains, averaging about 0.06 millimetres in diameter, and heavy minerals, mainly zircon and ilmenite with some tourmaline and apatite. The heavy minerals are especially abundant in the lower siltstones, where they congregate in laminae several millimetres apart and comprise up to 1 per cent of the rock; they are less abundant and more highly disseminated in the upper siltstones. The matrix of these beds consists mainly of cryptocrystalline calcite, with chlorite and muscovite in very small grains and in larger

FIGURE 4. Plot of the logarithm of siltstone thickness versus percentage cumulative frequency on probability paper. Plot is based on 167 measurements from member B in the area southeast of the Athabasca River.

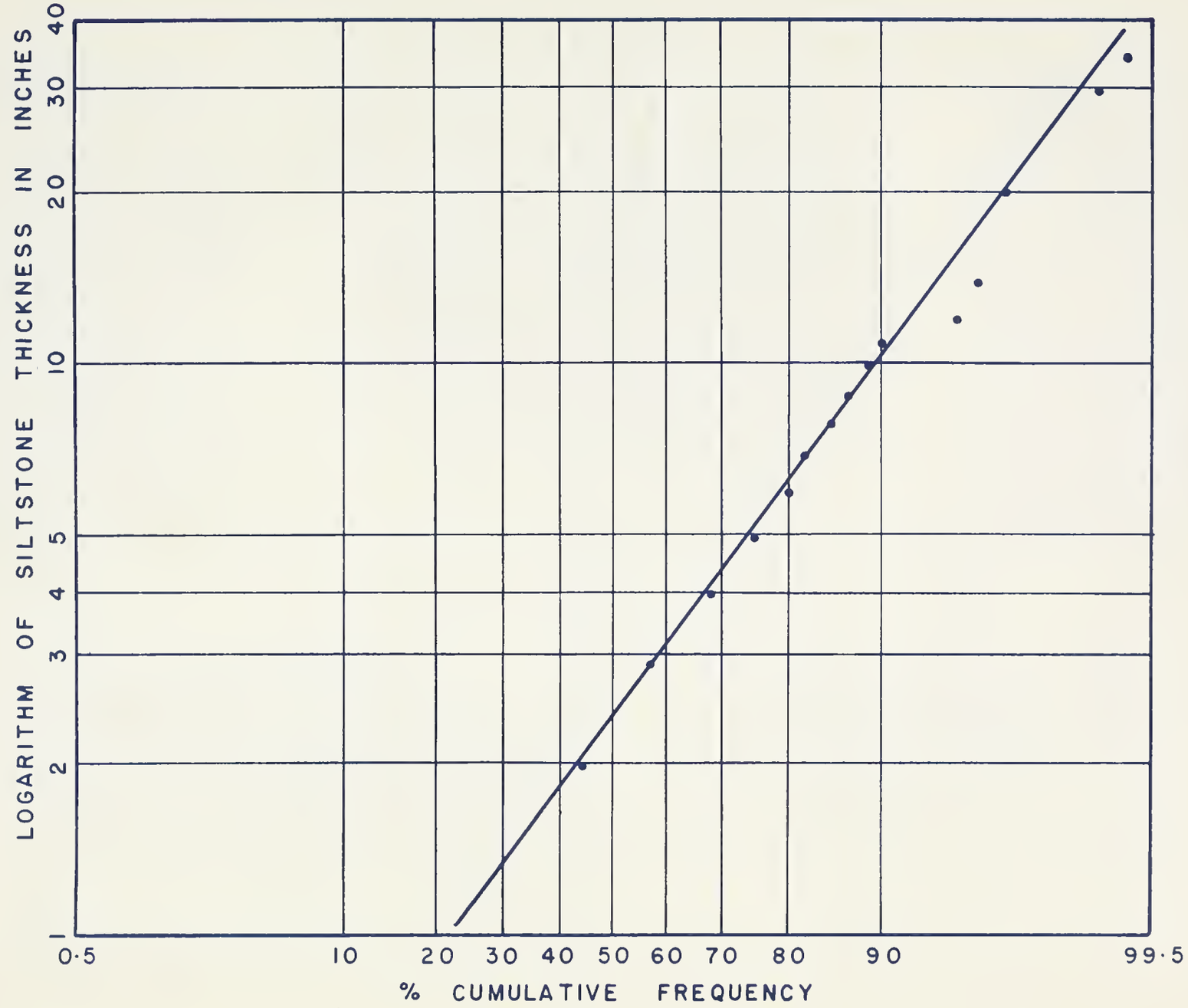
LOGARITHM OF SILTSTONE THICKNESS IN INCHES
40
30
20
10
5
4
3
2
1
0·5
10
20
30
40
50
60
70
80
90
99·5
% CUMULATIVE FREQUENCY

FIG·4

PLATE I

a. Cliff-forming intraformational limestone-breccia unit in the lower part of member B, near Old Fort Point.

b. Intraformational limestone-breccia from the upper part of member B near sub-area E. Phenoclasts are subparallel to bedding. Scale is in inches.

c. Basal beds of member B exposed in a road outcrop at Old Fort Point. The way up can be determined from scour and from the relationship between bedding and cleavage in the argillites. The beds marked "B" are thought to be bottomset, and those marked "F", foreset.

d. Pinch-and-swell structure or sedimentary boudinage of siltstone. From the type-section of member B north of Old Fort Point. Actual size.

e. Cross-stratification in the uppermost siltstones of member A, southeast of Old Fort Point. Scale is in inches.

a

b


c

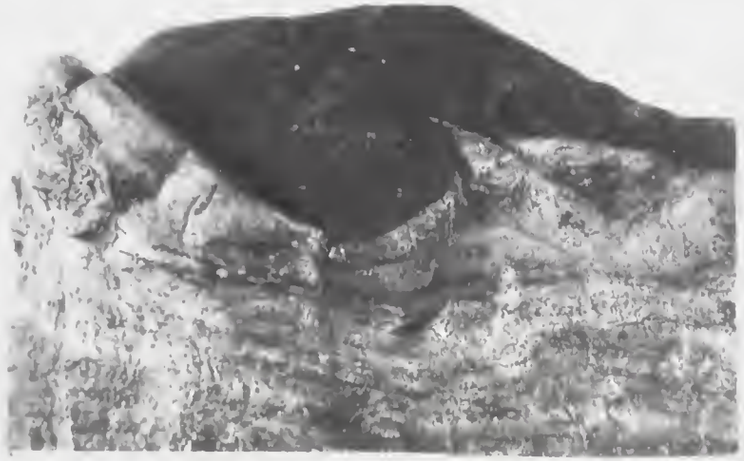

d

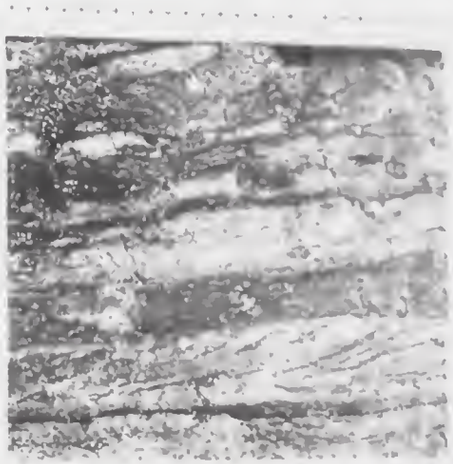

e

PLATE I

a. Cliff-forming intraformational limestone-breccia unit in the lower part of member B, near Old Fort Point.

b. Intraformational limestone-breccia from the upper part of member B near sub-area E. Phenoclasts are subparallel to bedding. Scale is in inches.

c. Basal beds of member B exposed in a road outcrop at Old Fort Point. The way up can be determined from scour and from the relationship between bedding and cleavage in the argillites. The beds marked "B" are thought to be bottomset, and those marked "F", foreset.

d. Pinch-and-swell structure or sedimentary boudinage of siltstone. From the type-section of member B north of Old Fort Point. Actual size.

e. Cross-stratification in the uppermost siltstones of member A, southeast of Old Fort Point. Scale is in inches.

a

b

c

d

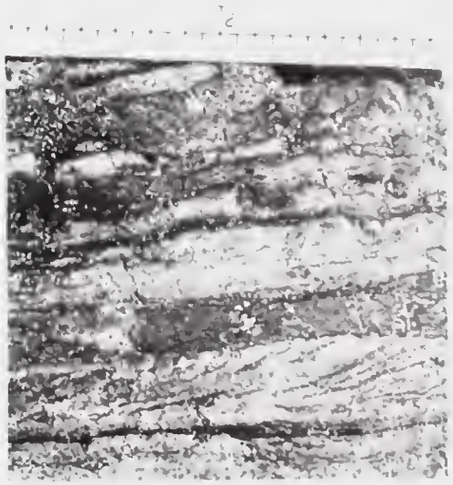

e

books, and minute rhombs of siderite. As well as decreasing in amount towards the top of the member, the matrix becomes progressively more calcareous, until at the top it consists almost entirely of crystalline twinned calcite.

Member C. Although member C is remarkably uniform lithologically, its thickness varies considerably. While the type-section, about one mile southeast of the bridge (Figures 1 and 2), displays some 250 feet of this member, only 90 feet is present just west of Jasper. The member consists of the following lithologies:

Argillite. The dark bluish grey, faintly laminated argillites of member C weather rusty brown. They are composed mainly of fine-grained chlorite and muscovite parallel or subparallel to cleavage. Silt-sized grains of quartz account for 10 to 20 per cent of the rock while somewhat larger books of chlorite with interlayered muscovite make up an additional 5 to 15 per cent. Up to 5 per cent of the rock may consist of minute siderite rhombs. Altered biotite is present as flakes in silt laminae and in some chlorite-muscovite books.

Quartzose Limestone-Breccia. A 10-foot quartzose limestone-breccia occurs near the top of member C in the southern and western parts of the map-area. This rock exhibits the curious association of up to 30 per cent dark bluish grey limestone phenoclasts in a matrix of coarse-grained calcareous sandstone. The phenoclasts contain up to 15 per cent silt-

sized albite with some quartz, in a groundmass of cryptocrystalline calcite and argillaceous material. The coarse quartz and albite grains of the breccia matrix were originally well rounded, but are now covered by irregular overgrowths, which project into the surrounding cryptocrystalline argillaceous and calcareous material.

Several feet of dark bluish grey, thin-bedded limestone similar to the phenoclasts of the breccia underlies this bed in the southwestern part of the area. Neither the limestone nor the quartzose limestone-breccia is present to the northeast, but the latter may be equivalent to a thin sandstone similar to the matrix of the breccia found near the top of member C near the type locality of member D (Figure 2).

Member D. The type section of member D and its location a half mile northeast of Old Fort Point, are shown in Figures 1 and 2 respectively. The main lithology is silty to sandy, greenish and bluish grey argillites which become coarser grained near the top of the member. Thin beds of fine-grained, olive grey, micaceous sandstone grade into bluish grey argillaceous siltstones. Dark bluish grey nodules up to 10 inches in diameter are randomly orientated in a 10 foot zone near the middle of the type-section. The surrounding material is poorly cleaved argillaceous siltstone and silty argillite. Although the association of chlorite, muscovite, quartz and albite present in the lower members is continued in member D, the olive grey sandstones are much richer in biotite than

any other rock-type observed in the Old Fort Point formation. The contact of this member with the overlying Miette formation was defined as the base of the lowest quartz pebble-conglomerate.

Conditions of Deposition. The strata of the Old Fort Point formation seem to record the building of a delta, so that conditions of deposition can best be described in terms of topset, foreset, and bottomset beds. The lower argillites of member A were probably deposited in fairly deep water some distance seaward of the approaching delta. The approach of the delta is marked by the increasing amount of silt near the top of member A. Small scale sedimentary structures such as those shown in Plate I e indicate a source to the northeast.

The transition from bottomset beds to foreset beds can be seen near the base of member B in the road outcrop at Old Fort Point. If the beds marked "B" in Plate I c were flat-lying, then beds "F" were deposited with an original dip of about 10 degrees northwest. The overlying sequence of breccias shown in Figure 6 supports this conclusion, although the average angle between foreset and bottomset beds is probably less than 10 degrees. The large breccia lens drops 110 feet in the half mile between section 9 and section 3 of Figure 3, thus making an angle of about 2 1/2 degrees, measured in a west-northwesterly direction, with the top of member A. Less direct evidence as to the inclined nature of the depositional surface of member B is present in the form of certain

FIGURE 5. Measured sections at the localities shown in Figure 2.

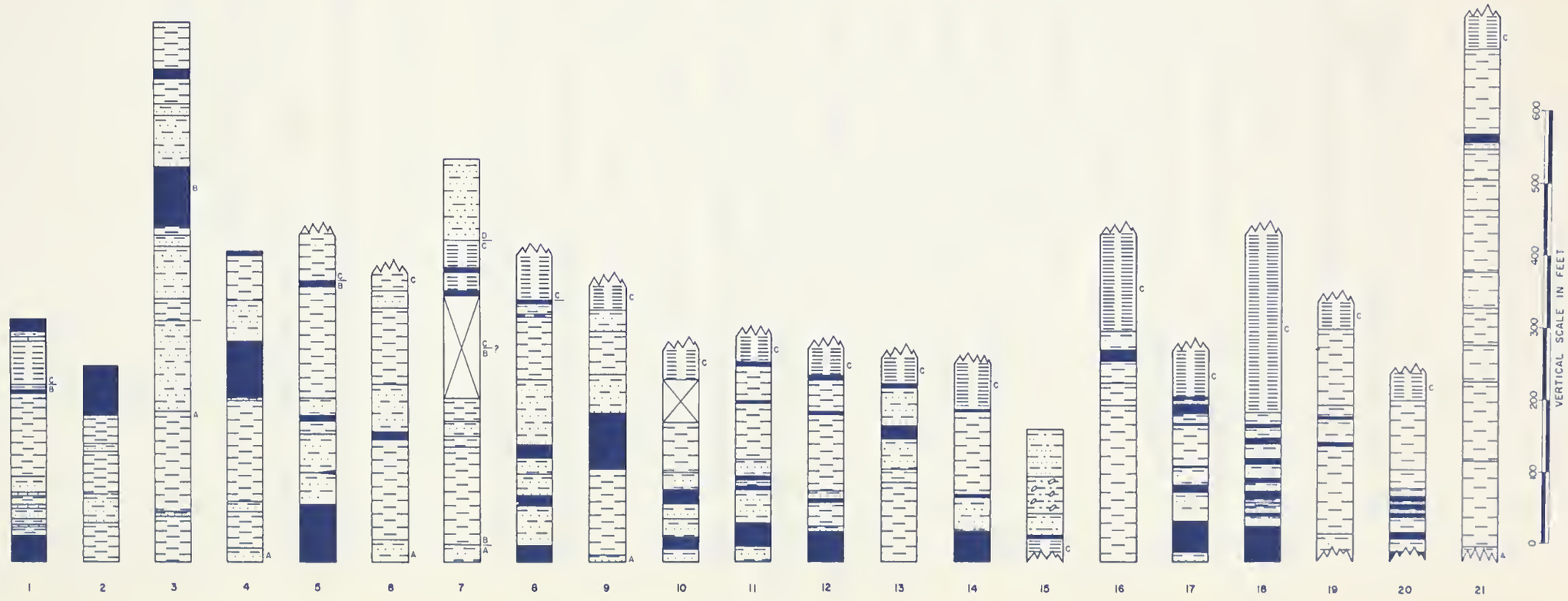
C
B
A
1
2
3
4
5
6
7
8
9
10
11
12
13
14
15
16
17
18
19
20
21
0
100
200
300
400
500
600
VERTICAL SCALE IN FEET

Figure 5

sedimentary structures, for although slump structures have been experimentally produced on non-sloping surfaces (Kuenen and Migliorini, 1950, p. 99), it is difficult to imagine a mechanism which could transport the large phenoclasts of the breccia units on such a surface. Other structures such as the slump in the limestone bed of Plate III g and the pinch-and-swell structure or sedimentary boudinage of Plate I d may have been produced by a westerly downslope movement.

The uniform argillaceous nature of member C suggests a return to quieter deposition. It is impossible to say whether this is due to regional subsidence or to a shift in the distributary system. The rapid thickening of this member to the northeast is also unexplained. Near the end of member C time, limestone was once more deposited in the area. The absence of these beds and the limestone breccia from the northeast part of the map-area is attributed to erosion by a turbidity current which deposited quartzose limestone breccia on top of the limestone in the southwestern part of the area. The coarse-grained sand thus deposited probably came from the topset beds of the next delta to encroach upon the area.

Member D, like member A shows the approach of shallow water deposition by the increased amount of silt and fine sand near the top, which finally gives way to coarse-grained sandstone and quartz pebble-conglomerate of the conformably overlying Miette formation. The beds of this member probably represent the final phase of the transition from

FIGURE 6. Large scale map of the road outcrop at old Fort Point, showing the lenticularity of the nearly vertical beds.

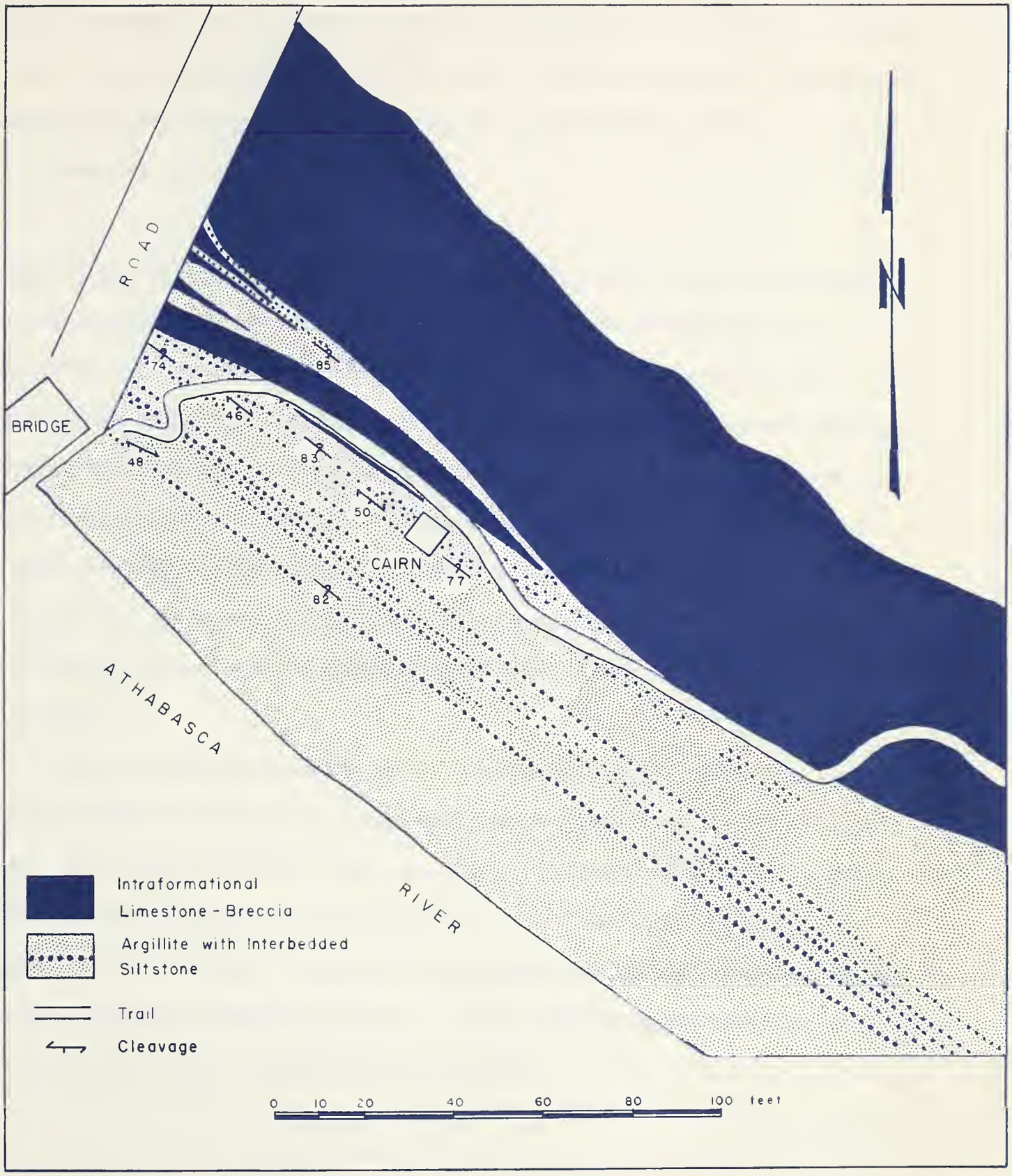
ROAD
BRIDGE
N
74
85
46
48
83
50
CAIRN
77
82
ATHABASCA
RIVER
Intraformational
Limestone - Breccia
Argillite with Interbedded
Siltstone
Trail
Cleavage
0 10 20 40 60 80 100 feet

FIGURE 6

relatively deep water deposition to the laying down of the Miette shallow water deposits (Remington, 1960, p. 23). In making the above interpretations the author was greatly aided by the work of Rich (1951, pp. 1-20), who deserves mention at this time.

Correlation with Other Areas. The Old Fort Point formation outcrops at several localities in the Miette River valley west of Jasper, where the succession is essentially the same as that found in the southwestern part of the map-area. Outcrops of member B consist of green and purple argillites overlain by thin-bedded limestones. Member C lithologies are represented by a quartzose limestone-breccia and blue iron-stained slate; however, this member has thinned to about one tenth the thickness measured at the type locality. The green argillites of member D grade into sandstone and quartz pebble conglomerate of the overlying Miette formation.

The Old Fort Point formation may be correlated with the type section of the Hector formation, commonly regarded as upper Proterozoic in age, near Lake Louise (Walcott, 1910, p. 428). Although individual Old Fort Point members can not be distinguished in this section, the lithologic similarity is striking. Green and purple argillites are associated with siltstones and limestone breccias. A quartzose limestone-breccia, containing large quartz pebbles is also present.

# TECTONICS

Introduction. The Precambrian strata of the Jasper area, which are assumed to have undergone deformation during the Laramide orogeny, are situated in the thrust-sheet of the Pyramid fault which outcrops in Pyramid Creek, 3 miles north-northeast of the town of Jasper, Alberta. Where the trace of this fault, which trends north 60 degrees west, crosses the Athabasca River, rocks of the Jasper formation are thrust over Devonian strata. Within the thrust-sheet, the older, less competent Old Fort Point and Miette formations are presently displayed in a series of tight anticlinoria and synclinoria, while the younger, more competent strata are usually gently dipping. The Jasper anticlinorium, whose axial trace passes through the town of Jasper, Alberta, exposes some of the oldest and most highly deformed rocks of the area.

Folding and Faulting. Within the Old Fort Point formation of the Jasper anticlinorium are a number of tight folds, most of which are overturned towards the northeast (Figure 7). The maximum observed horizontal distance separating successive anticlines is about 1500 feet, and the maximum structural relief about 1000 feet. The corresponding values for the overlying Miette formation to the west are 2500 feet and 3500 feet, respectively, while in the Jasper formation and Lower Cambrian quartzites, folds of this order of magnitude appear to be absent. Northwest of the Athabasca River the anticlinorium trends about north 70 degrees west,

FIGURE 7. Geological map of the Old Fort Point formation of the Jasper anticlinorium.

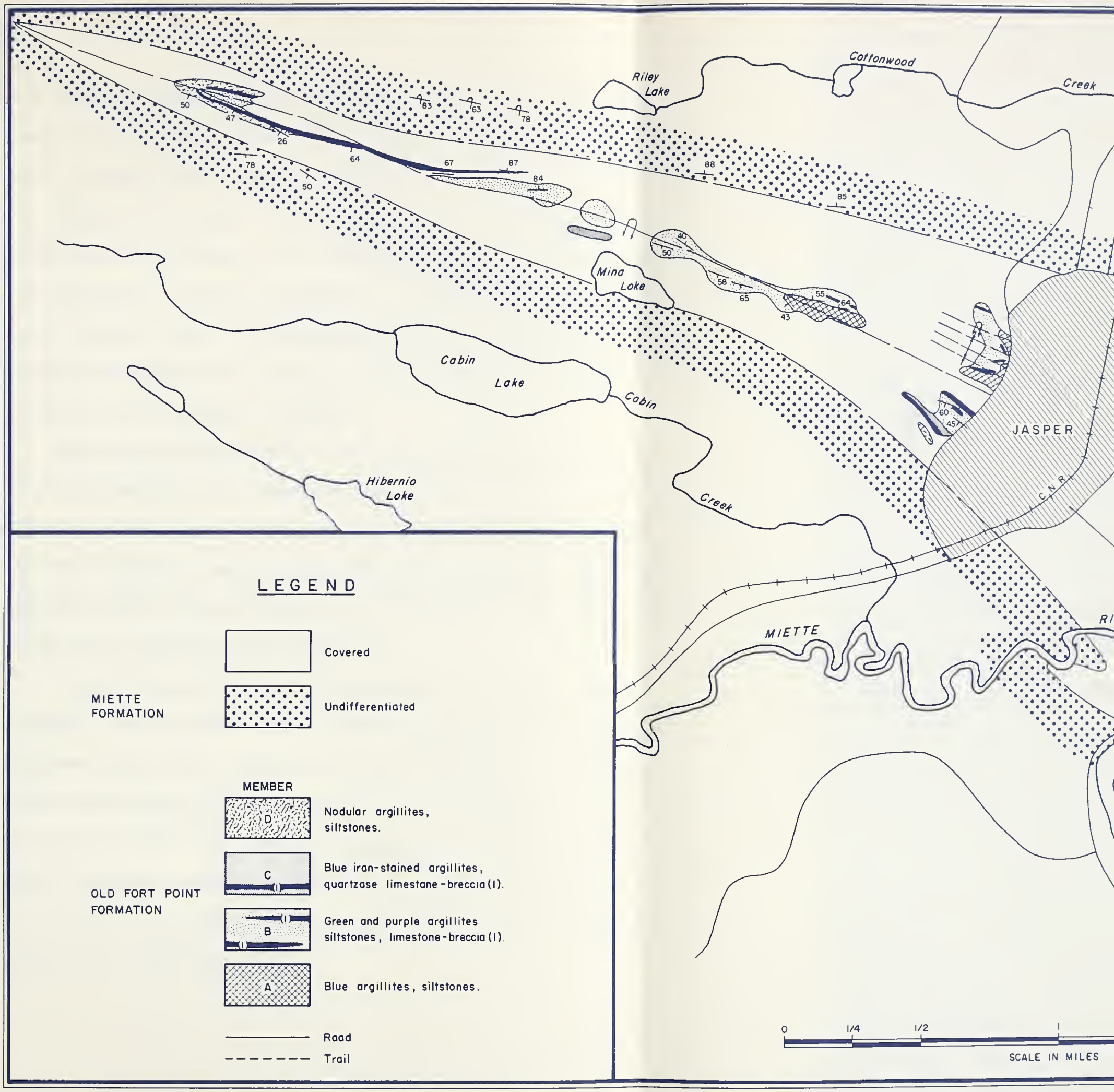


## LEGEND

Covered

MIETTE FORMATION — Undifferentiated

OLD FORT POINT FORMATION

MEMBER

D — Nodular argillites, siltstones.

C — Blue iran-stained argillites, quartzose limestone-breccia (I).

B — Green and purple argillites siltstones, limestone-breccia (I).

A — Blue argillites, siltstones.

Road

Trail

Figure 7

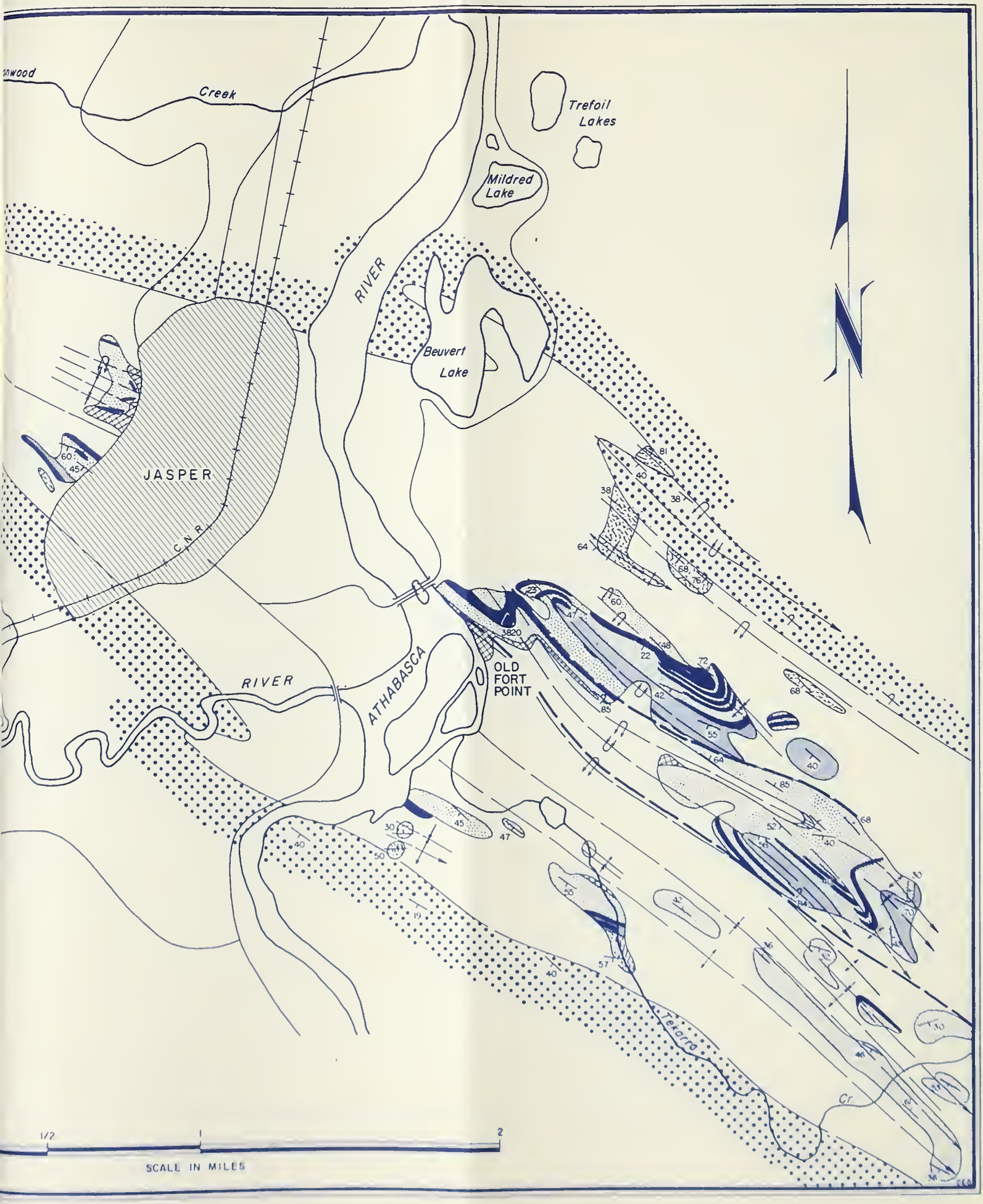
Creek
Trefoil Lakes
Mildred Lake
RIVER
Beuvert Lake
JASPER
C.N.R.
RIVER
ATHABASCA
OLD FORT POINT
Tekarra
Cr
1/2
1
2
SCALE IN MILES

Figure 7

and plunges northwest at angles ranging between 6 and 22 degrees. Immediately southeast of the river the trend is north 48 degrees west, with individual folds plunging anywhere between 32 degrees northwest and 12 degrees southeast. Half a mile southeast of the river, all observable folds plunge to the southeast at angles varying between 5 and 25 degrees, and either maintain or steepen this plunge in the extreme southeast part of the map-area. The axial planes of folds, determined by measuring the attitude of flow cleavage (see below), dip between 65 and 75 degrees southwest.

While the style of folding in the Old Fort Point formation is largely dependent on the competency of the beds involved, individual folds are almost certainly disharmonic. Where folds are developed in the more incompetent parts of the succession, the folding tends to be similar, whereas folding tends to be of the parallel type in the case of the more competent strata (Figure 8).

A relatively small amount of deformation was achieved through faulting. Two high-angle thrust-faults were observed in the overturned, northeast limbs of two adjacent anticlines (Figure 9). Displacement along these faults is probably small near the Athabasca River, but seems to increase towards the southeast, carrying to the surface strata which would otherwise be buried because of the steep plunge. Plate II a depicts ruptured siltstones in the axis of a syncline which have undergone rupture instead of folding.

FIGURE 8. Diagrammatic structural cross-sections, the locations of which are in Figure 2.

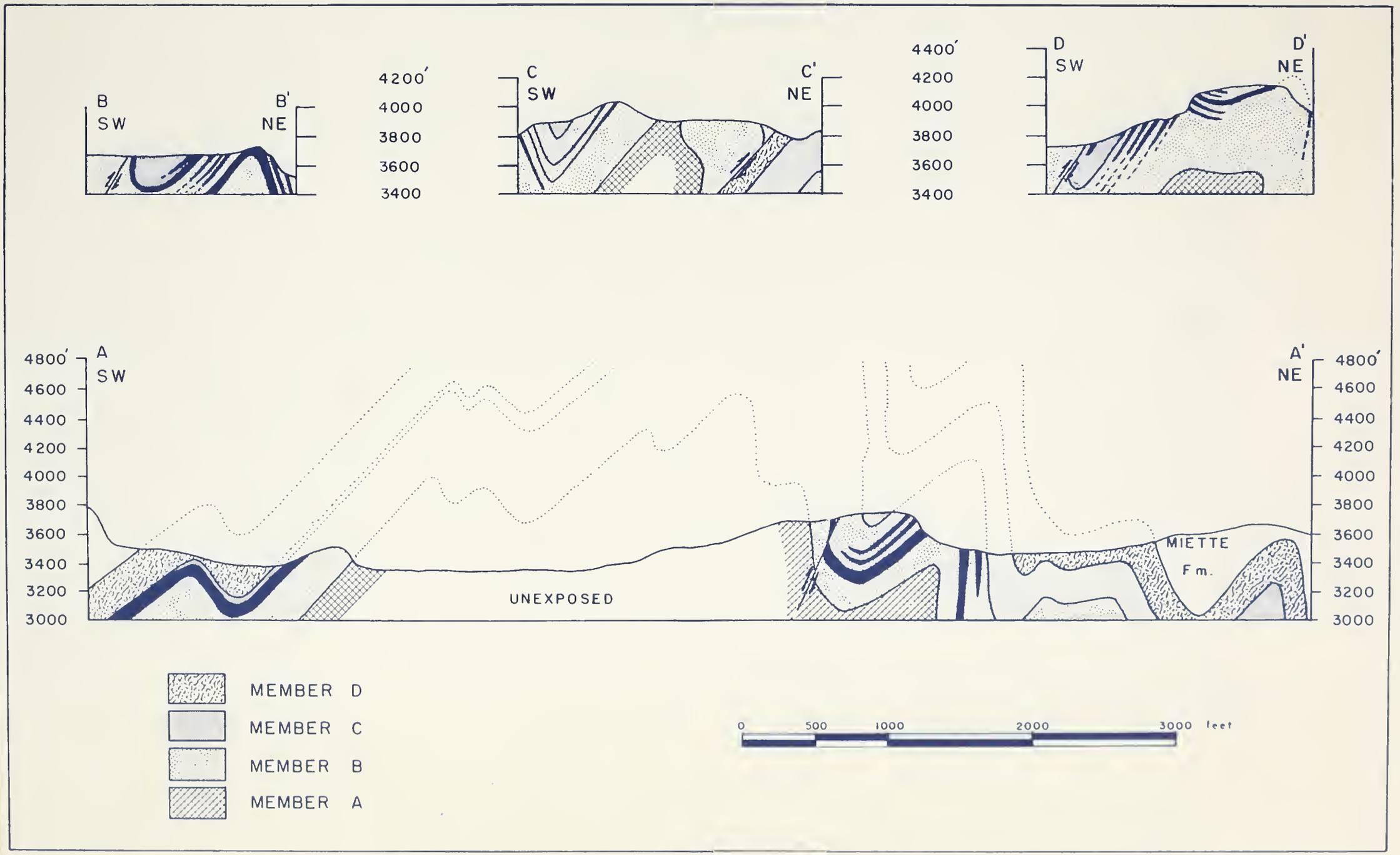
B
SW
B'
NE
4200'
4000
3800
3600
3400
C
SW
C'
NE
4400'
4200
4000
3800
3600
3400
D
SW
D'
NE
A
SW
A'
NE
4800'
4600
4400
4200
4000
3800
3600
3400
3200
3000
UNEXPOSED
MIETTE
Fm.
MEMBER D
MEMBER C
MEMBER B
MEMBER A
0
500
1000
2000
3000 feet

FIGURE 8

FIGURE 9. Geological map of the Old Fort Point formation in the vicinity of Old Fort Point.

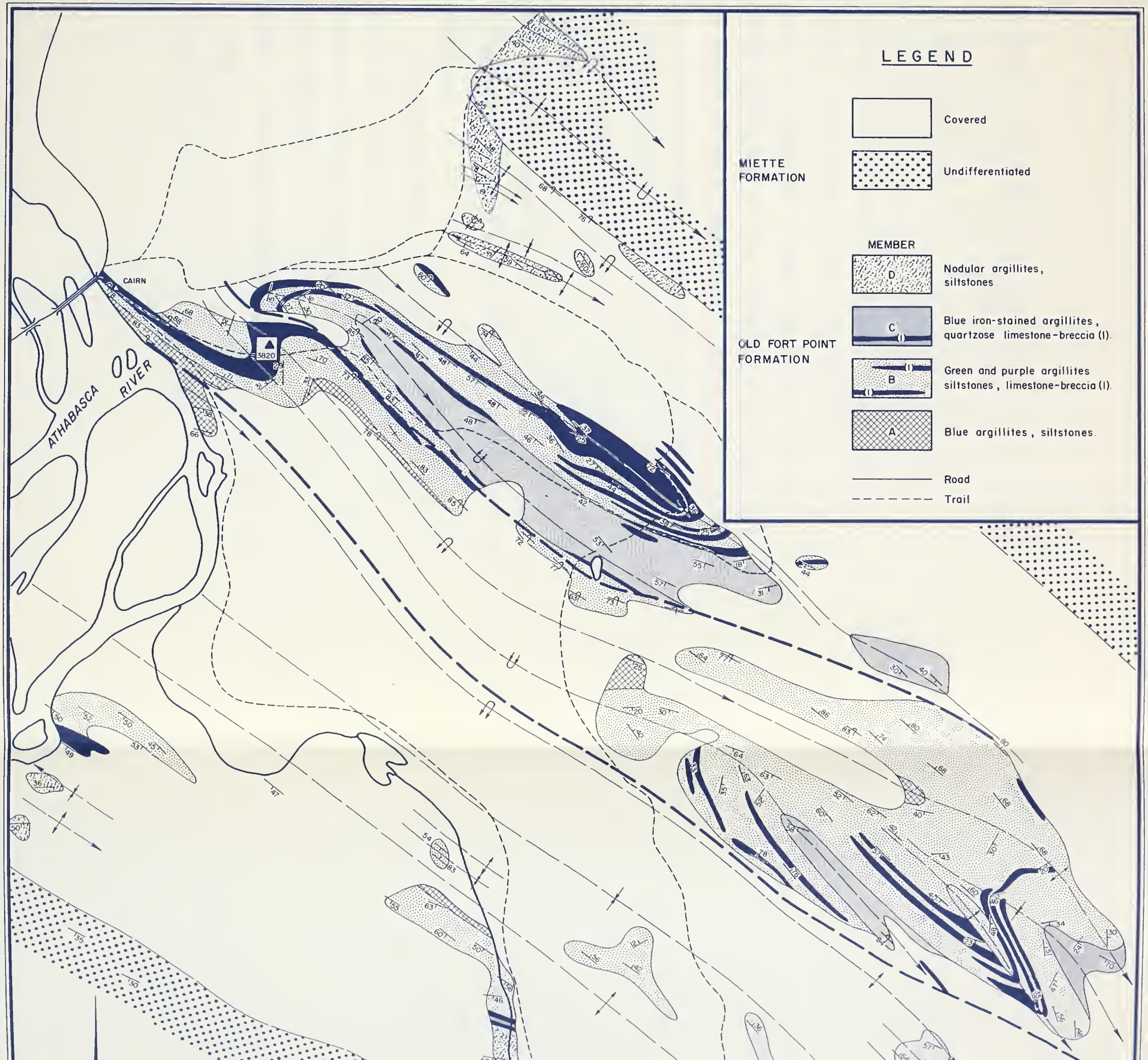
LEGEND
Covered
MIETTE FORMATION
Undifferentiated
MEMBER
D
Nodular argillites, siltstones.
C
(I)
Blue iron-stained argillites, quartzose limestone-breccia (I).
OLD FORT POINT FORMATION
B
Green and purple argillites siltstones, limestone-breccia (I).
A
Blue argillites, siltstones.
Road
Trail
CAIRN
3820
ATHABASCA
OD
RIVER

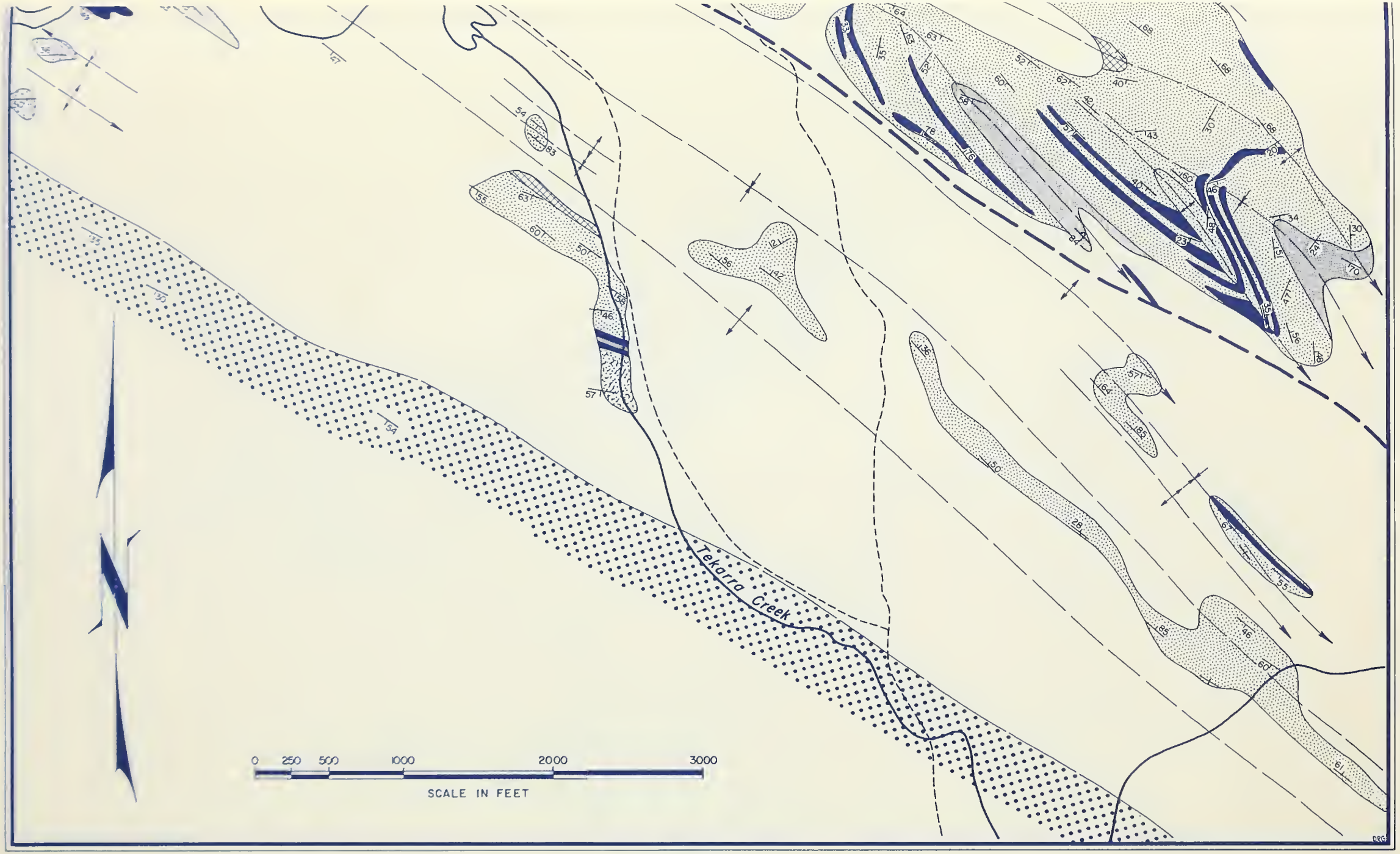


Figure 9

Cleavage. Flow-cleavage is well developed in the incompetent argillites, but stops abruptly at the contacts with the more competent siltstones and breccias (Plate II b). Attitudes of both cleavage and bedding were noted at 152 localities in the map-area southeast of the Athabasca River (Figure 10). The poles to about 140 cleavage planes were plotted on a Schmidt equal-area net, differentiating between the readings taken on the northeast and southwest limbs of anticlines (Figure 10 a). The modal plunge of the poles on the northeast and southwest limbs is about 40 and 20 degrees northeast respectively, suggesting that cleavage is arranged in a fan-like manner about the axial planes of folds. The accompanying rose-diagram based on all 152 readings shows the distribution of aximuth of cleavage poles (Figure 10 b). The apparent polymodal character may represent variation in the structural trend within the relatively small area studied. In this case the corresponding frequency diagram from a larger area, but with the same number of points, would probably be much smoother.

The dip of cleavage was plotted against the dip of bedding at 80 localities (Figure 11). Since flow cleavage is very sensitive to the presence of competent beds (see below), the data for this comparison were taken from argillites of members A, B, and C with as little siltstone as possible. As can be seen from Figure 11, the average value for dip of cleavage along fold-axes is about 70 degrees southwest. While the dip increases at the rate of 2 degrees for every 10 degree increase in dip

FIGURE 10. Cleavage map of the area southeast of the Athabasca River.

10 a. Poles to 140 cleavage planes plotted on a Schmidt equal-area net.

10 b. Rose diagram of the bearing of 152 cleavage poles.

Figure 10b

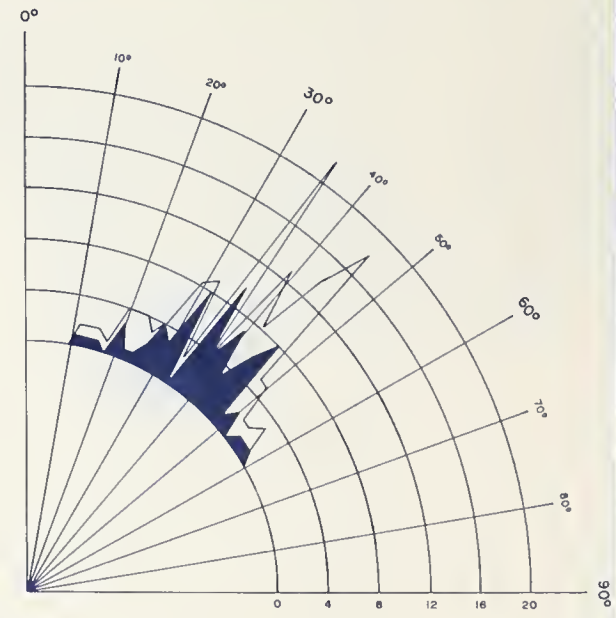


SW LIMBS OF ANTICLINES
NW LIMBS OF ANTICLINES
(2° CLASSES) (152 READINGS)

14 / 67 CLEAVAGE DIPPING 67° IN BEDS PLUNGING 14°

ATHABASCA RIVER

MIETTE

OLD FORT POINT

3822

Figure 10a
CLEAVAGE POLE PLOT

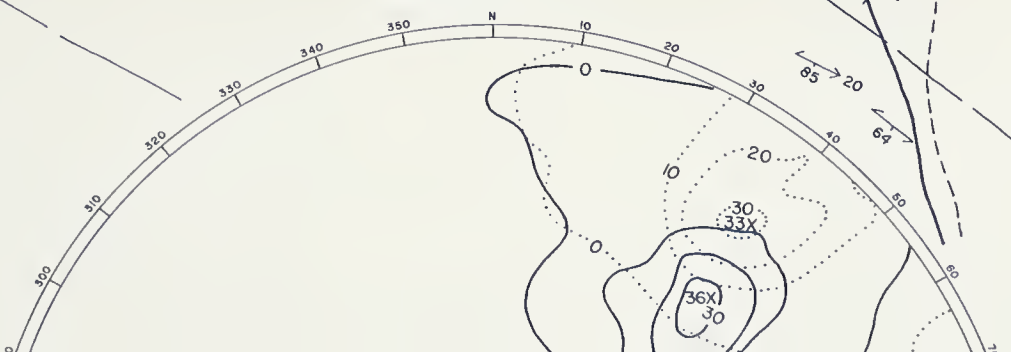

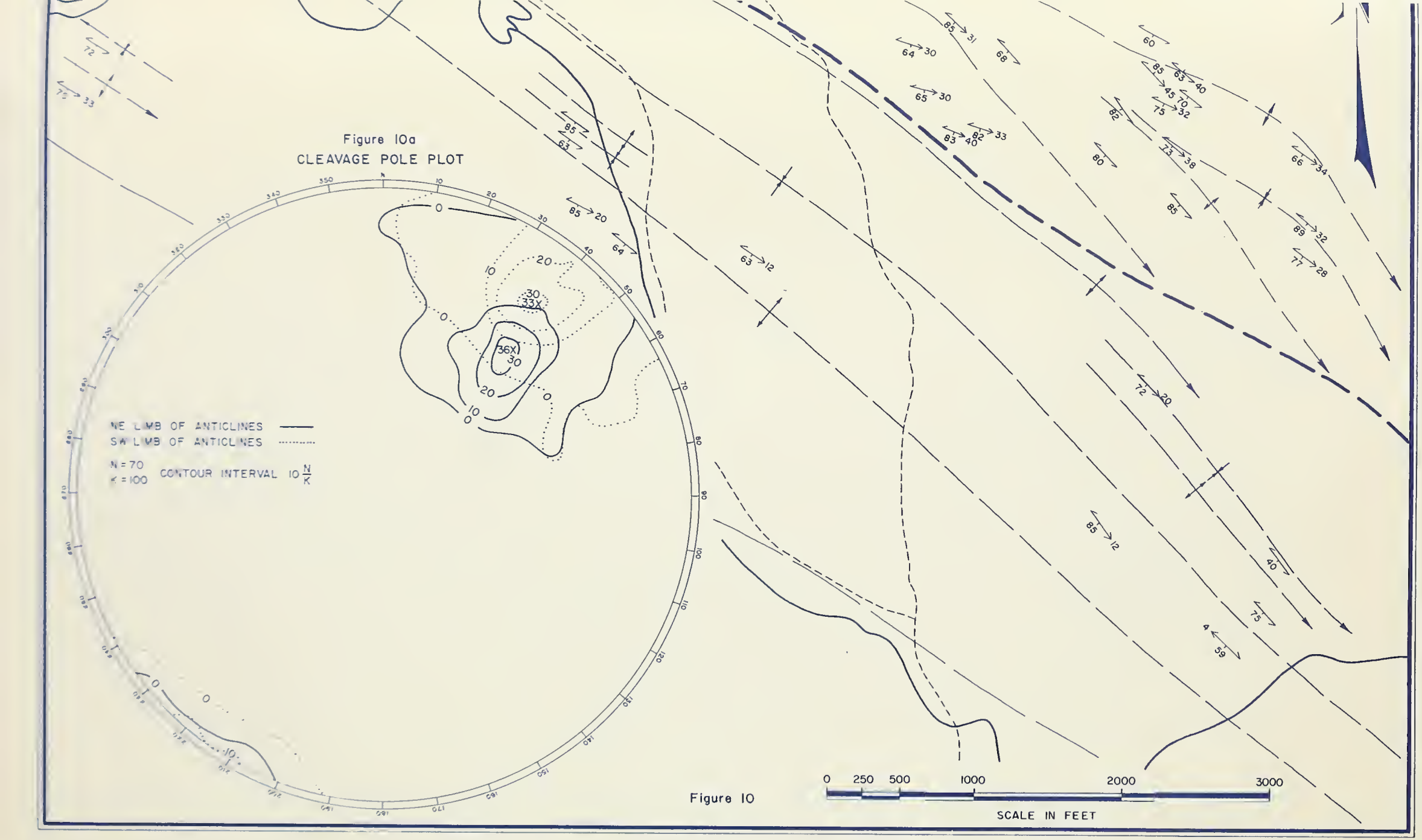
Figure 10a
CLEAVAGE POLE PLOT
NE LIMB OF ANTICLINES
SW LIMB OF ANTICLINES
N = 70
K = 100
CONTOUR INTERVAL 10 N/K
0
10
20
30
33X
36X
0 250 500 1000 2000 3000
SCALE IN FEET

Figure 10

FIGURE 11. Plot of flow-cleavage dip versus dip of bedding.

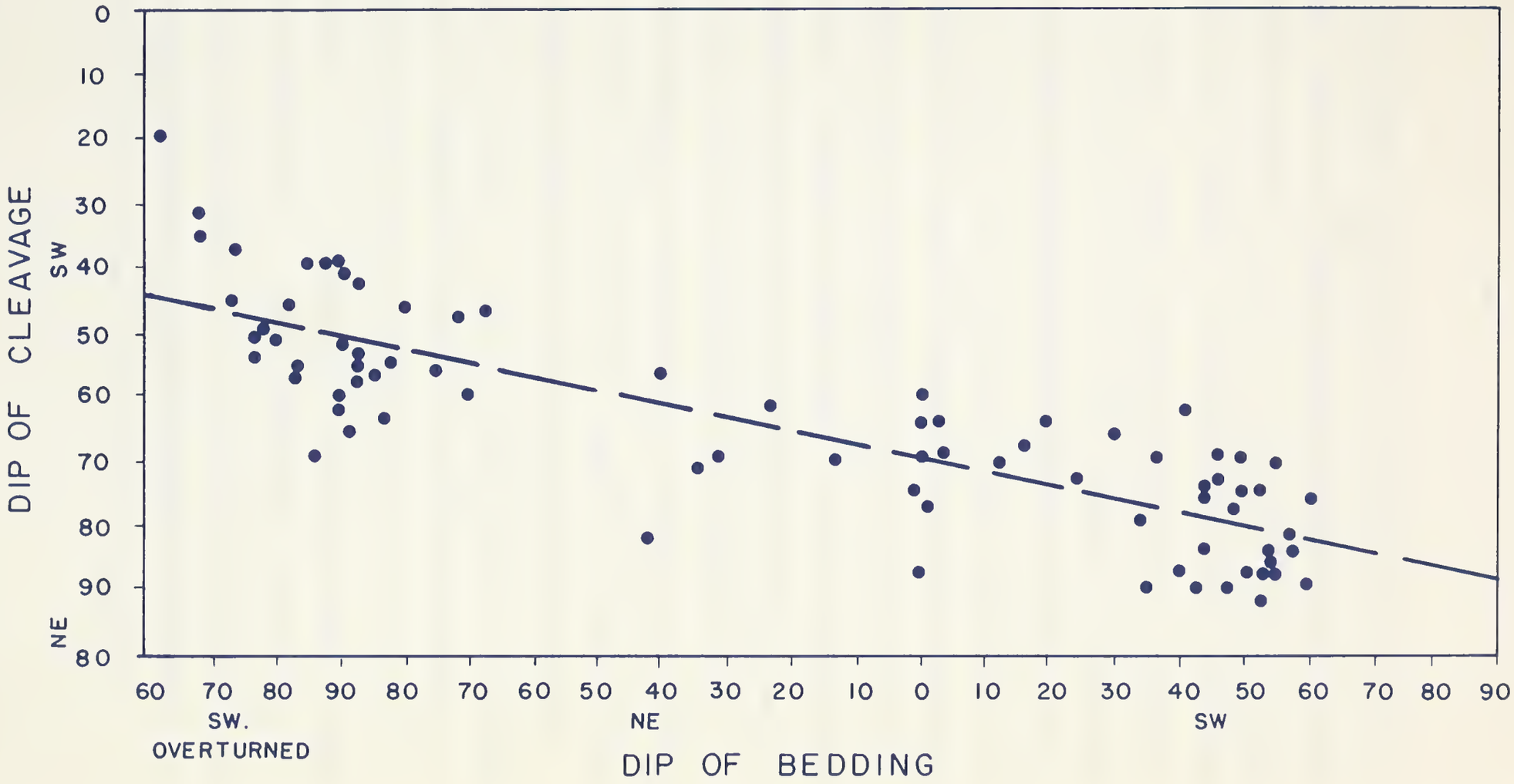
DIP OF CLEAVAGE
0
10
20
30
40
50
60
70
80
90
80
SW
NE
60 70 80 90 80 70 60 50 40 30 20 10 0 10 20 30 40 50 60 70 80 90
SW.
OVERTURNED
NE
SW
DIP OF BEDDING

FIGURE 11

of bedding to the southwest, and decreases at the same rate for bedding dipping northeast, there is a 20 degree spread of points parallel to the ordinate. A similar spread was obtained in a study of cleavage developed in the incompetent beds of member C in the syncline east of Old Fort Point summit. It is therefore concluded that where the amount of interbedded siltstone is at a minimum in the Old Fort Point formation, cleavage can depart from a mean plane, controlled by the attitude of bedding and the orientation of the regional stress-field, by an angle usually less than 10 degrees. The amount of departure is probably a function of the percentage of competent material interbedded with the incompetent rocks in which the cleavage is developed; it thus might be almost zero in the case of a thick, uniformly incompetent formation, reaching a maximum where the incompetent units are thin and bounded by thick competent units.

The fan-like arrangement of cleavage about fold-axes may be accounted for in two ways. The so called "lag theory" suggests that the re-orientation of platy minerals perpendicular to the regional maximum principal stress lags behind the folding, so that upon stress-release the cleavage planes are frozen in a metastable position; or if the re-orientation of cleavage did keep pace with folding throughout most of the fold history, there was tightening of the folds after the cessation of cleavage development. The other theory points out that cleavage may be always perpendicular to the maximum stress applied to it, but the orientation of the local maximum principal stress-axis may vary throughout the fold due to the tendency of the rocks to transmit stress parallel to bedding.

Several examples of cleavage-fans which are the reverse to those postulated by the "lag theory" were observed in the area studied (Figure 12), but in every case the cleavage was perpendicular to the expected maximum principal stress-axis, suggesting that the latter assumption may be valid for this area.

The orientation of the stress-field within the interbedded competent and incompetent strata of member B probably varied considerably, providing an excellent opportunity to study the effect of stress-variation on cleavage. Figure 12 illustrates the attitude of cleavage within a one-foot band of incompetent argillite interbedded with two competent siltstone beds in a minor fold exposed on a joint-face approximately perpendicular to the fold-axis. Assuming there has been no tightening of the fold since the cessation of cleavage formation, the unbroken lines perpendicular to the cleavage represent the actual maximum principal stress-axes operative during folding. The broken lines indicate the average orientation of the maximum principal stress-axes in a fold of identical shape where the effect of the competent material is nil (see Figure 11). As can be seen, there appears to have been considerable rotation of the stress-field in the relatively thin argillite bed, a rotation which is ascribed to the differential movement between the overlying and underlying competent units in the directions indicated by the arrows. Presumably the effect of this differential movement at the centre of an incompetent bed decreases rapidly as its thickness increases until the amount of rotation is nil.

The cleavage in the northeast limb of the syncline in Figure 12 is sigmoidal, making an angle of about 45 degrees with the siltstone near the contacts, and curving to an angle of about 30 degrees near the centre of the argillite bed. This curvature, which is opposite to that which would be produced in post-cleavage folding, probably formed in response to a local stress-system, the origin of which is not understood.

Figure 13 shows cleavage planes wrapping around a small but relatively competent breccia lens in member C, exposed on a similar joint-face. Planes are everywhere perpendicular to the expected local maximum principal stress-axis, and the divergence of the cleavage away from the local high pressure zone, developed where the breccia lenses out, is entirely in keeping with its flow nature. The same effect was observed in member D, with concretions providing the competent, non-flowing material. In this case it was possible to observe the cleavage wrapping around both ends of the rigid obstruction.

Evidence of the flow nature of cleavage is not restricted to orientation analyses. Argillaceous material has flowed parallel to cleavage-planes into fractures in siltstone beds (see p. 56). In very well cleaved phyllitic beds, lineations can be seen in the cleavage plane (ab) paralleling the direction of transport (a).

Flow-Cleavage and Thickness Variation. If, during folding, the amount of material that moved parallel to cleavage is much greater than that which moved across the cleavage, it is possible to estimate the original

FIGURE 12. Probable stress variation in argillites near competent beds, as shown by the orientation of flow cleavage. Note the reverse fan-arrangement of cleavage. Sketch from photograph of Plate II b.

FIGURE 13. Cleavage planes wrapping around the pinch-out edge of a competent breccia lens exposed on a vertical joint-face. Sketch is from a photograph.

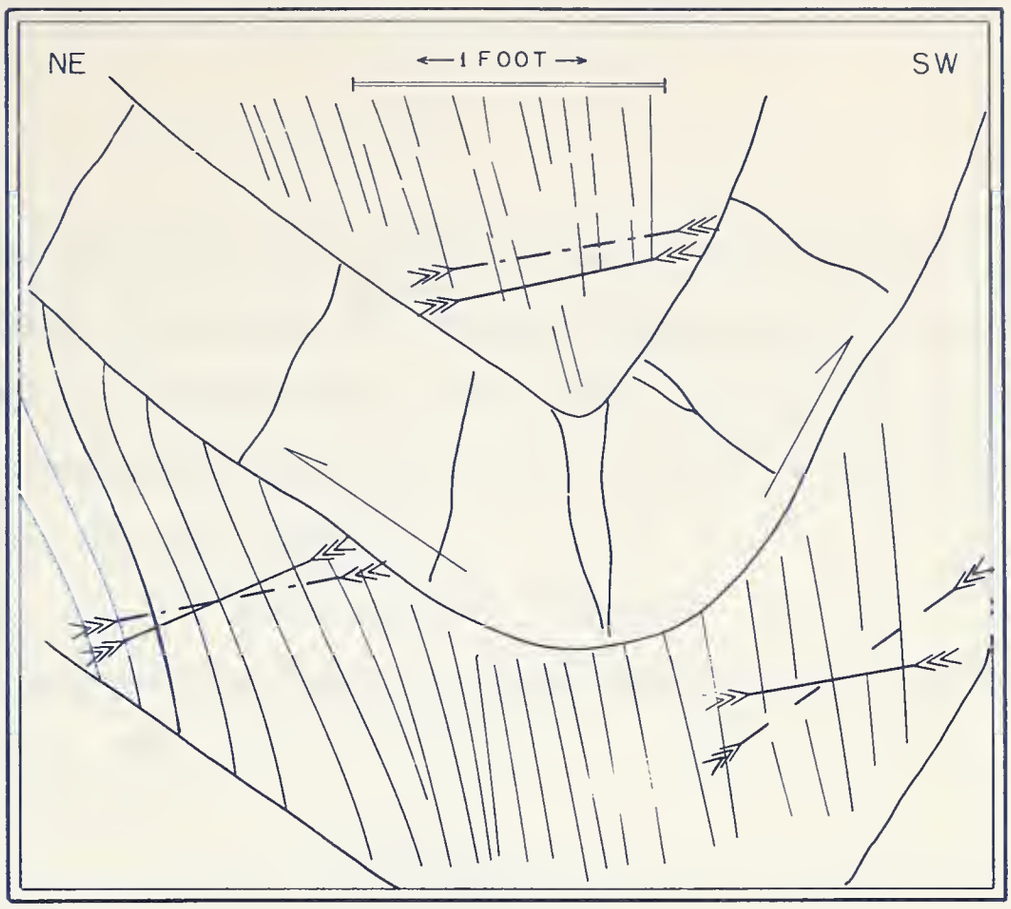


FIGURE 12

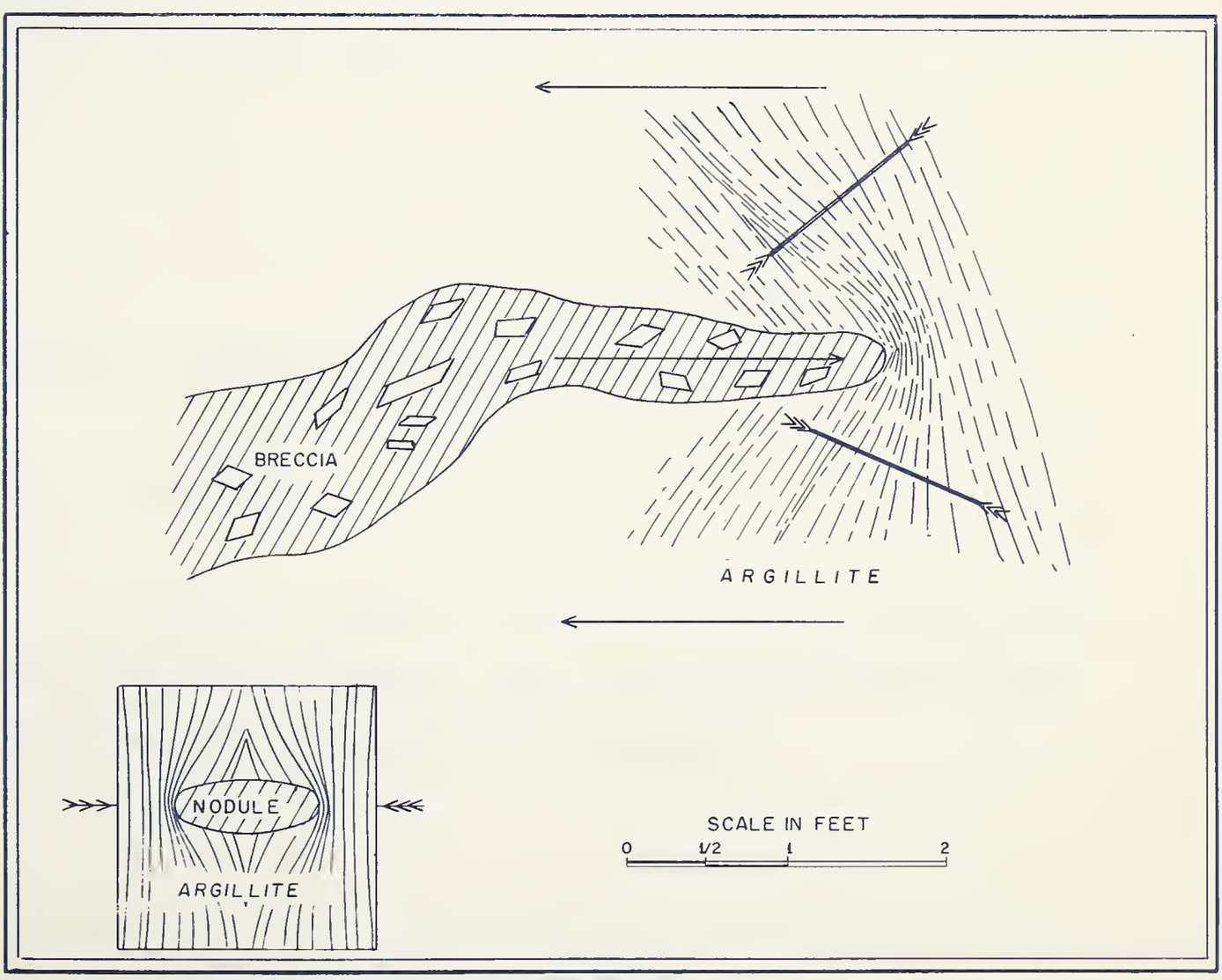


FIGURE 13

thickness of folded and cleaved strata. Assuming that an original sphere of radius r deformed to an ellipsoid having major semi-axes a, b, and c, parallel to the minimum, intermediate, and maximum principal stress-axes respectively, there having been a negligible change in volume (Billings, 1954, pp. 340-1),

$$4/3\,\pi\ r^3 = 4/3\,\pi\ a.b.c \qquad (1)$$

Since it is reasonable to assume that strain parallel to b can be ignored (Cloos, 1947, p. 863),

$$b = r \qquad (2)$$

therefore

$$r^2 = a \cdot c \qquad (3)$$

Deformation can thus be thought of as taking place in a plane perpendicular to b in which the sphere and ellipsoid appear as a circle and ellipse, respectively (Figure 14).

Let

$$r = 1 \qquad (4)$$

then

$$a \cdot c = 1 \qquad (5)$$

In order to simplify the following calculations, let

$$\frac{c}{r} = \delta \qquad (6)$$

then, by equation (4)

$$c = \delta \qquad (7)$$

It is now possible to estimate the original thickness of a bed ($T_1$) in terms of its observed thickness ($T_2$), a ratio of shortening ($\delta$), and the observed angle between bedding and cleavage $\theta$.

Let $$T_1 = r \tag{8}$$

then

$$T_2 = OT \tag{9}$$

where T is some point (x,z) on the ellipse,

$$\frac{x^2}{a^2} + \frac{z^2}{c^2} = 1 \tag{10}$$

Then

$$c^2x^2 + a^2z^2 = a^2c^2 \tag{11}$$

or

$$c^2 + \frac{a^2z^2}{x^2} = \frac{1}{x^2} \tag{12}$$

But

$$\frac{z^2}{x^2} = \cot^2 \theta \tag{13}$$

so that

$$x^2 = \frac{1}{c^2 + a^2 \cot^2 \theta} \tag{14}$$

and

$$z^2 = x^2 \cot^2 \theta \tag{14}$$

$$= \frac{\cot^2 \theta}{c^2 + a^2 \cot^2 \theta} \tag{15}$$

Therefore

$$\sqrt{x^2 + z^2} = \sqrt{\frac{1 + \cot^2 \theta}{c^2 + a^2 \cot^2 \theta}} \tag{16}$$

and

$$OT = \sqrt{\frac{1 + \cot^2 \theta}{\delta^2 + \frac{1}{\delta^2} \cot^2 \theta}} \quad (\theta \neq 0) \tag{17}$$

Since OT is the thickness of a deformed bed ($T_2$), which was originally one unit thick, the original thickness of any bed may be given by

FIGURE 14. Projection of a sphere and ellipsoid of equal volume on a plane perpendicular to bedding and cleavage. The b axis of the ellipsoid is perpendicular to the plane of the paper. The direction of flow is a, and the direction of shortening is c. b is perpendicular to a and c and parallels the fold-axes. The cleavage plane is ab. (Sander, 1930, p. 119).

FIGURE 15. Ratio of measured thickness ($T_2$) to original thickness ($T_1$), plotted against the angle between bedding and cleavage ($\theta$), for various intensities of deformation, or ratios of shortening ($\delta$). The angles between bedding and cleavage at which neither thickening nor thinning occurs in beds whose ratio of shortening is 0.7, 0.6, and 0.5, are a, b, and c, respectively.

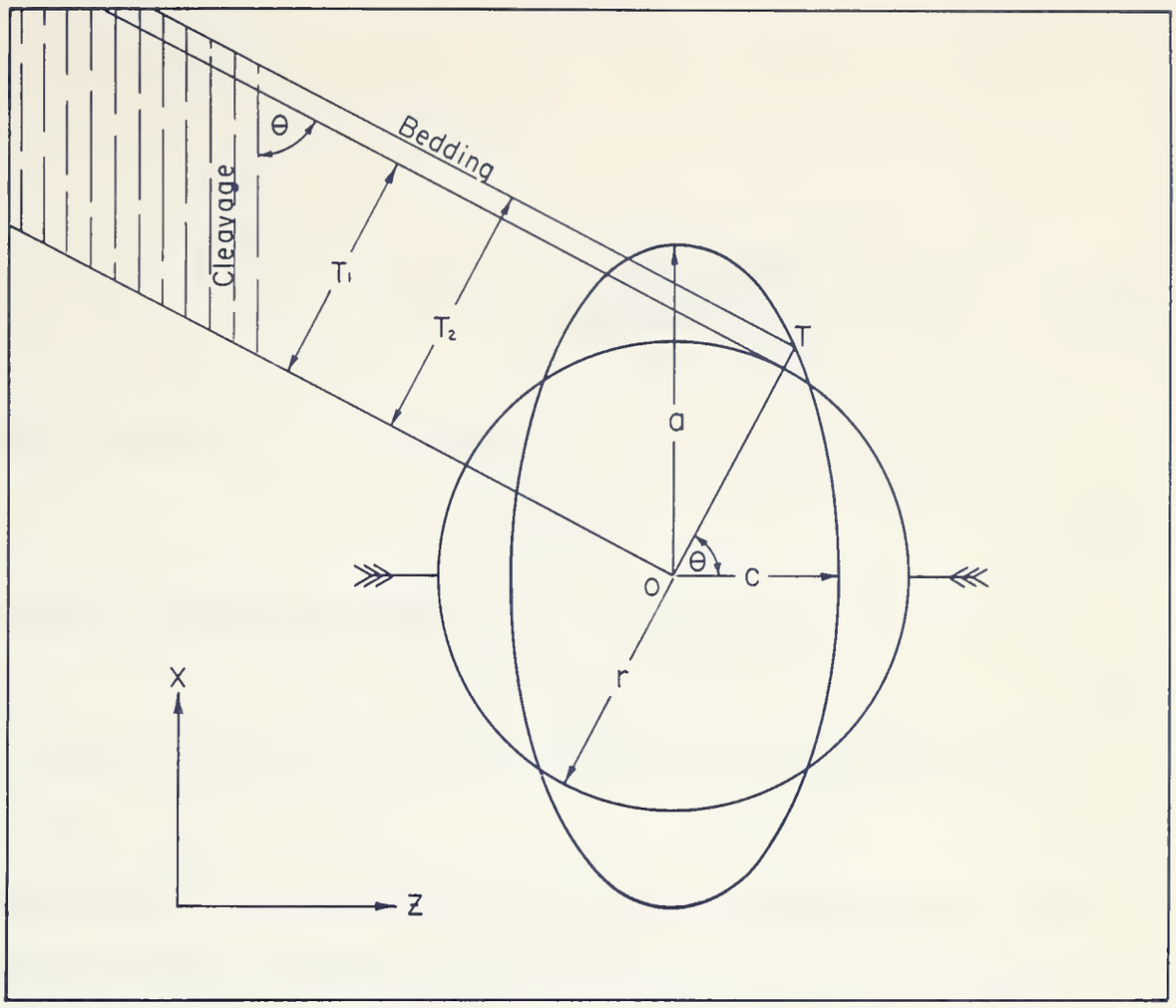


FIGURE 14

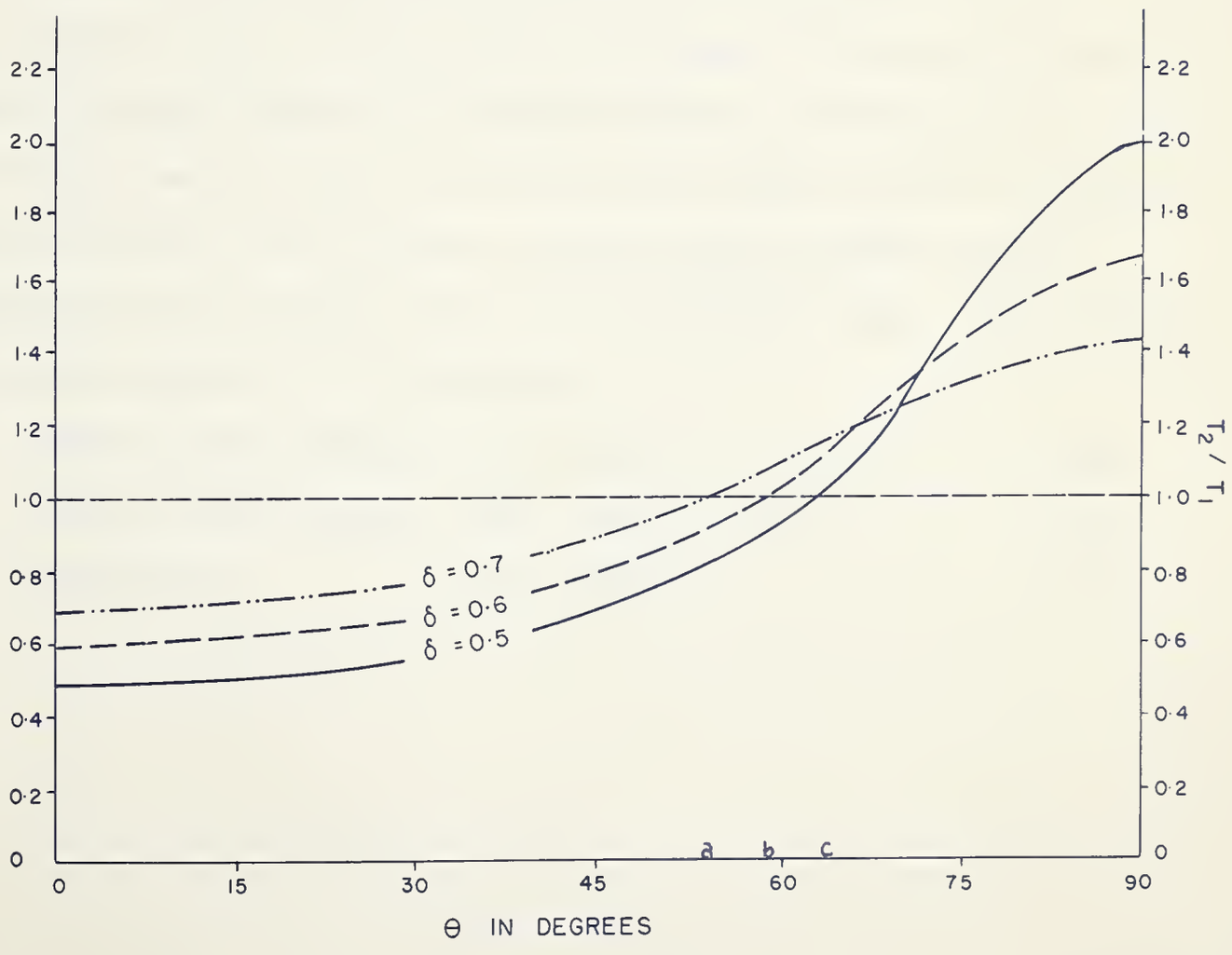


FIGURE 15

$$T_1 = \frac{T_2}{\sqrt{\frac{1 + \cot^2 \theta}{\delta 2 + \frac{1}{\delta^2} \cot^2 \theta}}} \quad (\theta \quad 0) \qquad (18)$$

The limiting value at $\theta = 0$ (bedding parallel to cleavage) is

$$T_1 = \frac{T_2}{\delta} \qquad (19)$$

and the limit with bedding perpendicular to cleavage is

$$T_1 = \delta T_2 \qquad (20)$$

Figure 15 shows the family of curves derived for $T_2/T_1$ with various values of $\delta$.

Estimation of $\delta$, the ratio of shortening, was based on a close examination of small-scale folds and other structures (see also p. 57). In Figure 16 the cross-sectional area of deformed argillite bounded by silt beds above and below and by synclinal axes to the right and left, was determined with a planimeter from a photograph. Because of the symmetrical boundary conditions, it seems reasonable to assume that this area has remained nearly constant during deformation, while the lack of thickening and thinning in the siltstones, indicates that the upper and lower boundaries have not changed length to any significant degree. The following calculations show how $\delta$ was estimated.

Length of upper boundary = 8.15 units. (21)

Length of lower boundary = 10.0 units. (22)

Measured Area = 7.9 units. (23)

FIGURE 16. Minor fold used to estimate the ratio of shortening ($\delta$). Sketch is from a photograph.

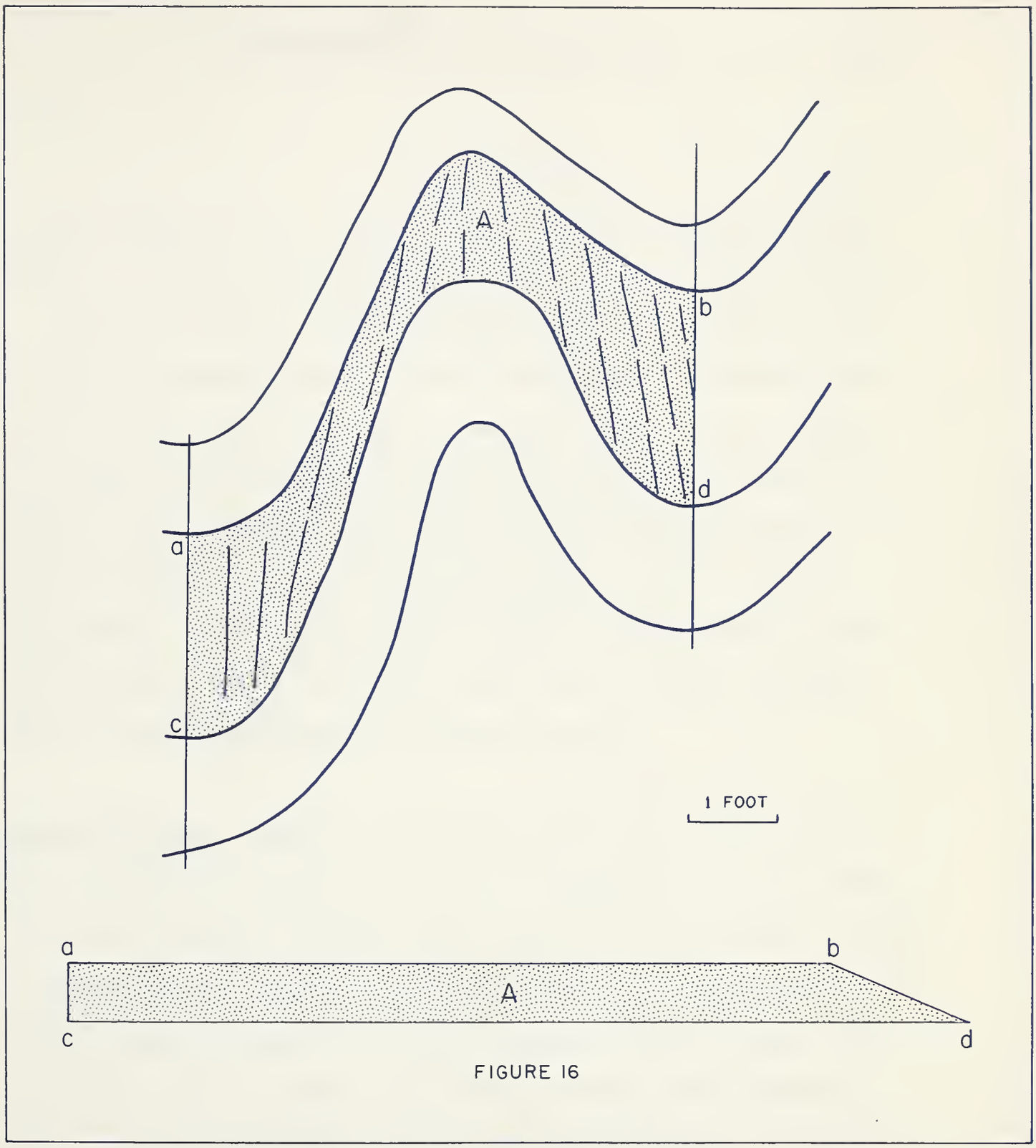


FIGURE 16

It follows that

$$\left(\frac{8.15 + 10.0}{2}\right) T_1 = 7.9 \text{ square units} \qquad (24)$$

so that

$$T_1 = 0.87 \text{ units} \qquad (25)$$

By using equation (20), a value for $\delta$ was found for each of the three fold-axes. These values from left to right are: 0.41, 0.67, and 0.40.

Small silt laminae, similar to those in Plate II c were also used to find $\delta$ by comparing their reconstructed original length with their present length. This method gives a maximum $\delta$-value since it measures the difference in shortening between the argillite and the thin silt laminae, rather than the absolute amount of deformation. Values obtained by this method vary between 0.70 and 0.85, thinner laminae giving higher values. A conservative estimate of the ratio of shortening in the area seems to be 0.70, so this value was used. The angle between cleavage and bedding was observed directly.

Fracture-Cleavage. The term fracture-cleavage as used here refers to closely spaced shear-fractures found in the competent siltstones. While the strike of fracture cleavage seems to parallel the fold-axes, the dip is dependent on the attitude of bedding (Figure 17). In the field, individual fractures appear to be spaced from 1/2 inch to 2 inches apart, but polished sections reveal the presence of numerous fine fractures paralleling the major ones. Fractures which do not extend to either

PLATE II

a. Ruptured siltstone beds of member B in a synclineal axis near the southeast corner of the map-area.

b. Minor fold exposed on a set 1 joint-face in sub-area C. Flow-cleavage terminates at the boundaries of the competent siltstone beds in which fracture-cleavage is developed (lower left). Joint set 1 has developed in the synclinal axis of the sharply flexed siltstone. See also Figure 12.

c. Ruptured silt laminae in member B argillite from sub-area C, used to estimate the ratio of shortening of the argillite. Note disharmonic flow folding controlled by the rupture pattern of the silt laminae.

d. Polished section of member B siltstone, showing the shear nature of fracture-cleavage.

e. Fracture cleavage in a siltstone from the top of member A. Flexing was followed by a small amount of displacement along this prefered fracture plane. Anticline is to left, syncline to right; bedding is nearly vertical.

a

b

c

d


e

PLATE II

a. Ruptured siltstone beds of member B in a synclineal axis near the southeast corner of the map-area.

b. Minor fold exposed on a set 1 joint-face in sub-area C. Flow-cleavage terminates at the boundaries of the competent siltstone beds in which fracture-cleavage is developed (lower left). Joint set 1 has developed in the synclinal axis of the sharply flexed siltstone. See also Figure 12.

c. Ruptured silt laminae in member B argillite from sub-area C, used to estimate the ratio of shortening of the argillite. Note disharmonic flow folding controlled by the rupture pattern of the silt laminae.

d. Polished section of member B siltstone, showing the shear nature of fracture-cleavage.

e. Fracture cleavage in a siltstone from the top of member A. Flexing was followed by a small amount of displacement along this prefered fracture plane. Anticline is to left, syncline to right; bedding is nearly vertical.

a

b

c

d


e

FIGURE 17. Graph showing the relationship between the dip of fracture-cleavage and the dip of bedding.

FIGURE 18. Cleavage-Boudinage in a 2-inch siltstone bed in member B. Sketch from a photograph.

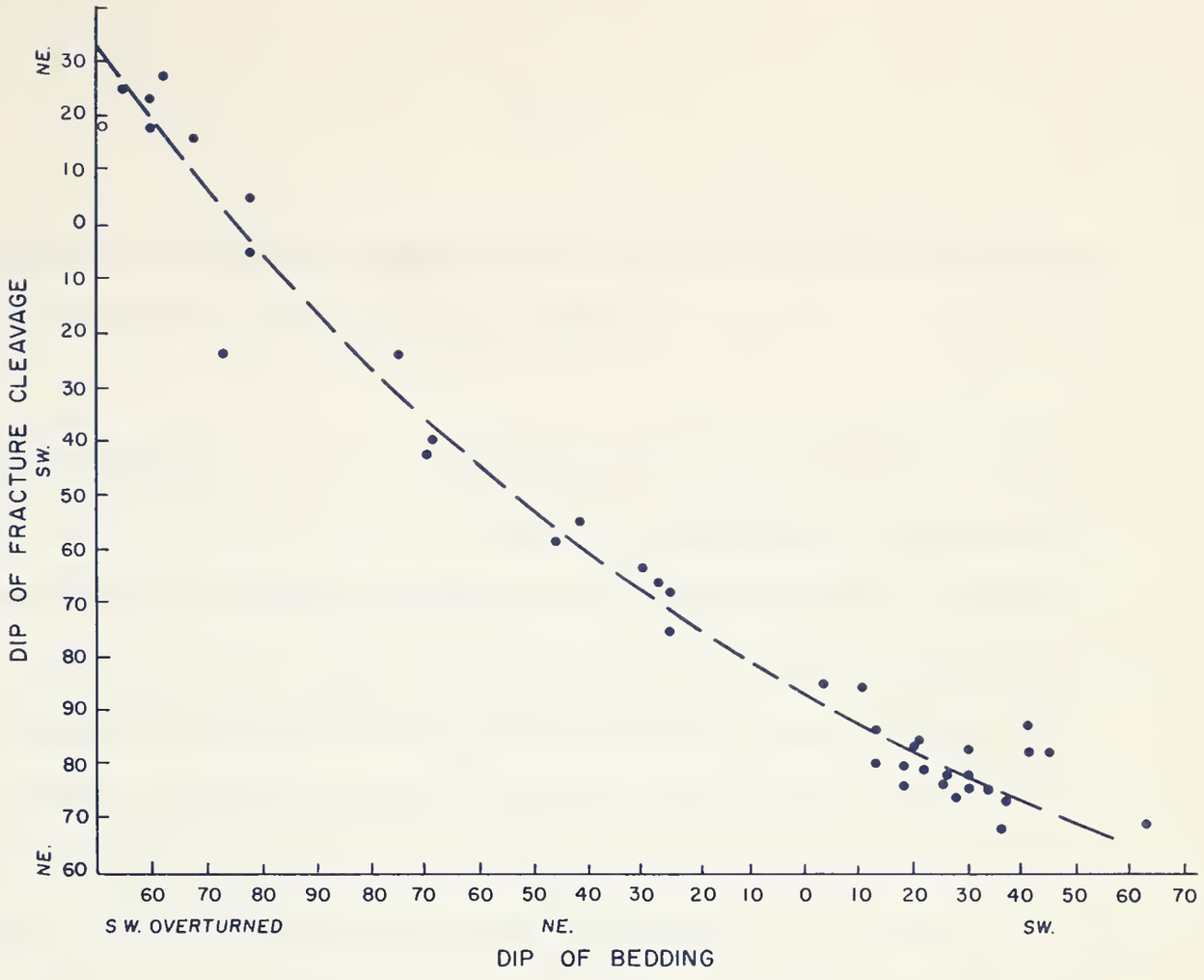


FIGURE 17

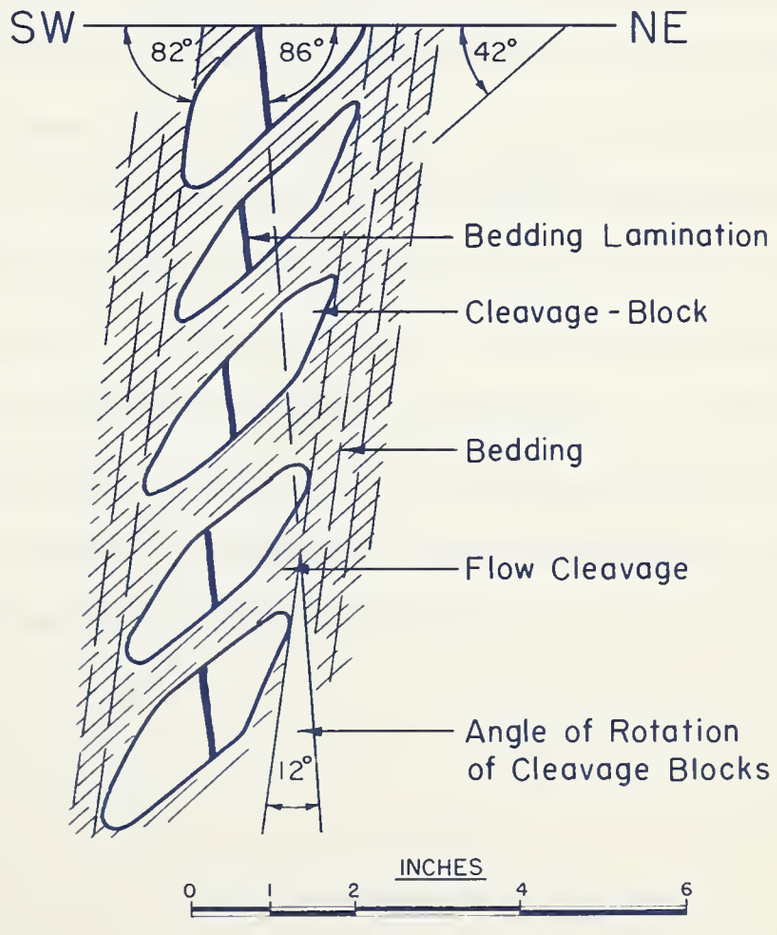


FIGURE 18

respect to bedding may be due to the presence of other stress-systems, internal rotation during folding, or both.

Cleavage-Boudinage. A type of cleavage-boudinage (de Sitter, 1958, p. 286), restricted to thin siltstones in predominantly argillaceous surroundings, is commonly present in the steeply dipping northeast limbs of anticlines. Figure 18 shows a 2-inch siltstone dipping 82 degrees southwest overturned which has developed cleavage-boudinage, being split up into a series of 1/2-inch cleavage-blocks dipping 42 degrees southwest, separated by 1/4-inch bands of cleaved argillaceous material. A small lamination within the silt bed dips 86 degrees northwest, indicating a 12 degree counterclockwise rotation of each boudin with respect to the surrounding bedding. The boudinage probably originated with the development of fracture-cleavage in the competent siltstone. During folding, the northeast limb of the anticline steepened, thus decreasing the angle between flow-cleavage and bedding in the surrounding argillites. Once this angle had decreased enough to produce thinning (Figure 15), further deformation was responsible for extension of the siltstone. This extension was effected not by continuous deformation or flowage as in the case of the cleaving argillites, but rather by the separation of cleavage-blocks or boudins by inflowing argillites from the adjacent beds. As well as separation, further deformation caused rotation of the boudins into a plane perpendicular to the maximum

principal stress-axis. Rotation ceased once the boudins reached this orientation. The present parallelism of the boudins to flow cleavage is thus another indication of the latter being a flow phenomenon.

Joints. Jointing is prominent in the tectonics of the Jasper anticlinorium. The poles to 180 joint-planes in the area southeast of the Athabasca River, when plotted on a Schmidt equal-area net, form a well-defined belt of points (Figure 19). For purposes of description, that part of the anticlinorium which has been most intensively studied has been divided into a number of sub-areas (Figure 2). In sub-area A the beds strike north 55 degrees west and dip 80 degrees southwest overturned, while the plunge ranges from horizontal to 12 degrees southeast. Sub-area B is structurally an overturned syncline, trending north 45 degrees west and plunging 30 degrees northwest, while sub-area C contains a relatively broad syncline with a similar trend and a plunge of 15 to 20 degrees southeast. The beds in sub-area D strike north 45 degrees west and dip 80 degrees southwest overturned. Sub-area E is situated close to the crest of an anticline which trends north 50 degrees west and plunges 25 degrees southeast.

It is possible to distinguish 9 joint-sets (Table I), each of which is described separately below. An attempt has been made to ascertain the genesis of each set and the orientation of the stress-field at the time of its formation. Inasmuch as rotation has often occurred, the original rather

TABLE I

| Set | Strike | Dip | Type | Period of Formation |
|---|---|---|---|---|
| 1 | N.38 E. | Vert. | Extension | Late or post-folding, pre-stress-release. |
| 2 | N.75 W. | 25 NE.# | Tension | Synchronous with folding. |
| 3 | N.-- S. | 30 E. # | Shear | Synchronous with folding. |
| 4 | N.45 E. | 20 NW.# | Shear | Synchronous with folding. |
| 5 | N.10 E. | 60 SE. | Shear? | Post-stress-release. |
| 6 | N.55 E. | 50 NW. | Shear? | Post-stress-release. |
| 7 | N.80 W. | 25 N. | Shear | Post-folding, pre-stress-release. |
| 8 | N.70 W. | 25 S. | Shear | Post folding, pre-stress-release. |
| 9 | N.15 E. | 30 W. | Shear? | Post folding. |

# Varies with bedding, values given are from sub-area A.

FIGURE 19. Field orientation of joints on a Schmidt equal-area net.

FIGURE 20. Inferred orientation of joints at their time of formation.

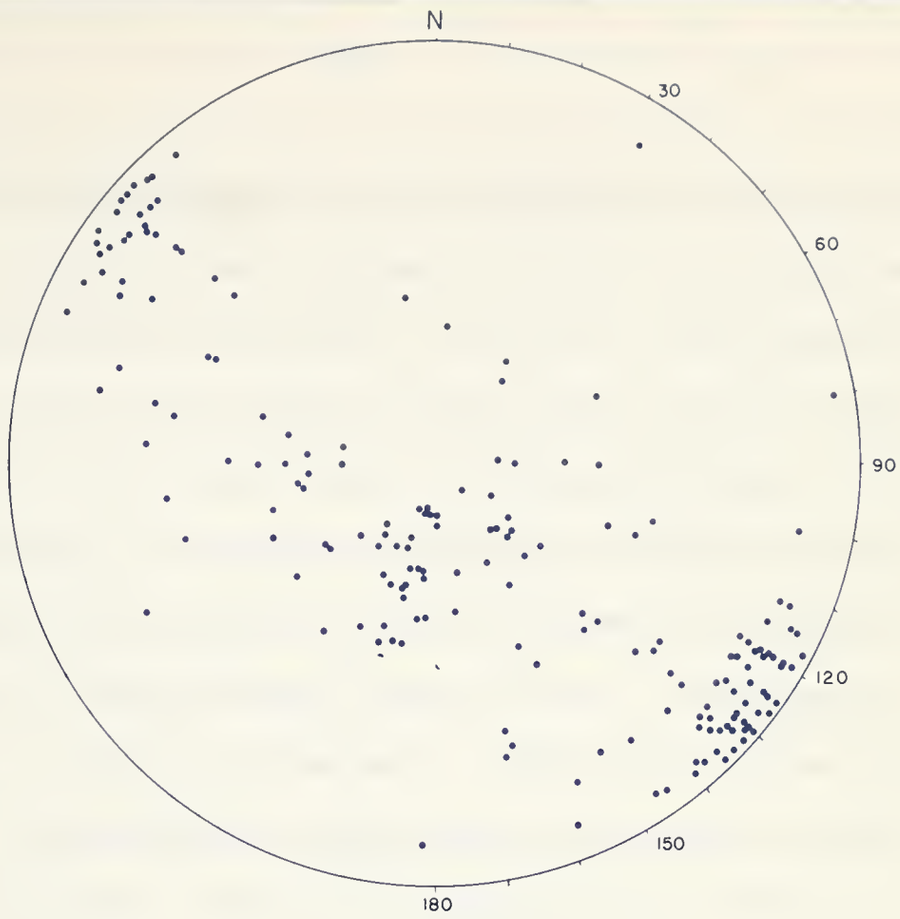


FIGURE 19

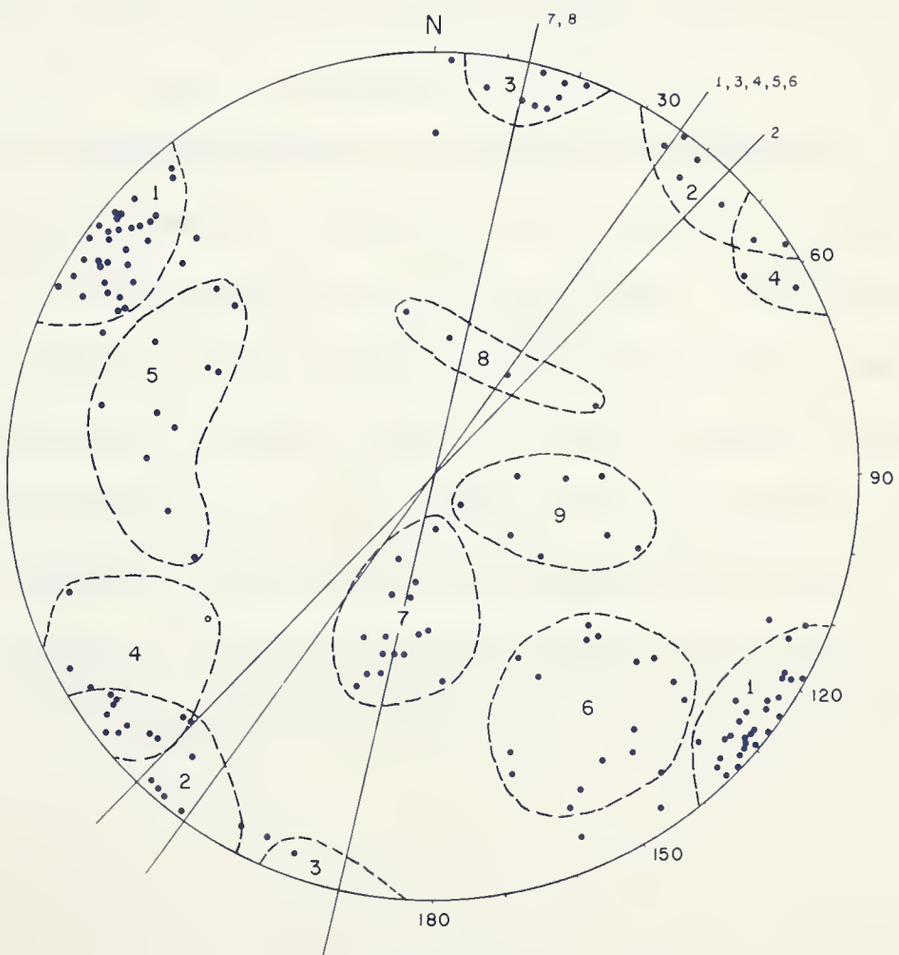


FIGURE 20.

than the present attitude of joints is of significance in this discussion. Joints which are thought to have originated before, or during the early stages of folding presumably developed in relatively flat-lying strata. Thus, in order to find their original attitude, they have been rotated in such a way that the beds in which they occur become horizontal. On the other hand, no rotation is necessary in the case of those joints which originated after folding; their present attitude is probably the original one.

The vertical to steeply dipping joints of set 1, perpendicular to the structural trend, are the most prominent. Cutting siltstone and argillites with little or no discrimination, these joints are smooth and almost never filled with vein material. The set is particularly well-developed in sub-area C where individual joints, slicing smoothly and uniformly through numerous minor folds, often attain an area of several hundred square feet. The joints are unevenly spaced, ranging from several feet to a few inches apart; some planes actually intersect at low angles (Plate III a). Examples of set 1 terminating against set 2 are present in sub-area A, indicating that set 1 was still developing after set 2 had formed. The presence of this set in well-cleaved argillite indicates that it was still forming after cleavage had ceased to develop, while its close relation to the local tectonic pattern indicates that it formed prior to stress-release. The dip of set 1 appears to be related to the plunge of the fold in which it occurs (Figure 21), while the strike (Figure 22) closely parallels the bearing of the maximum principal stress-axis as determined from flow-

FIGURE 21. Dip of joint-set 1 plotted against the plunge of the structure in which they occur.

FIGURE 22. Rose diagram of the strike of 74 joints of set 1 in the area southeast of the Athabasca River.

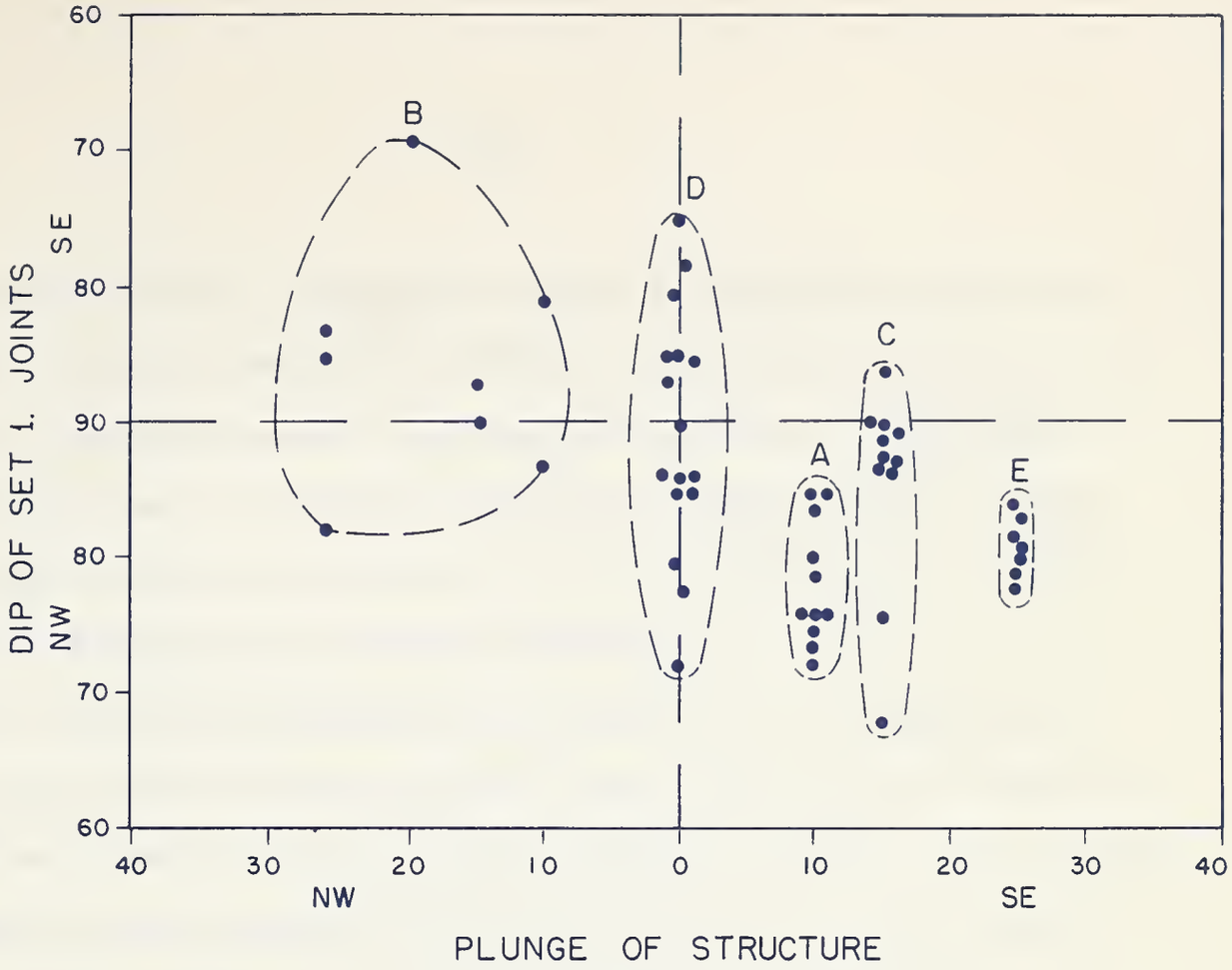


FIGURE 21

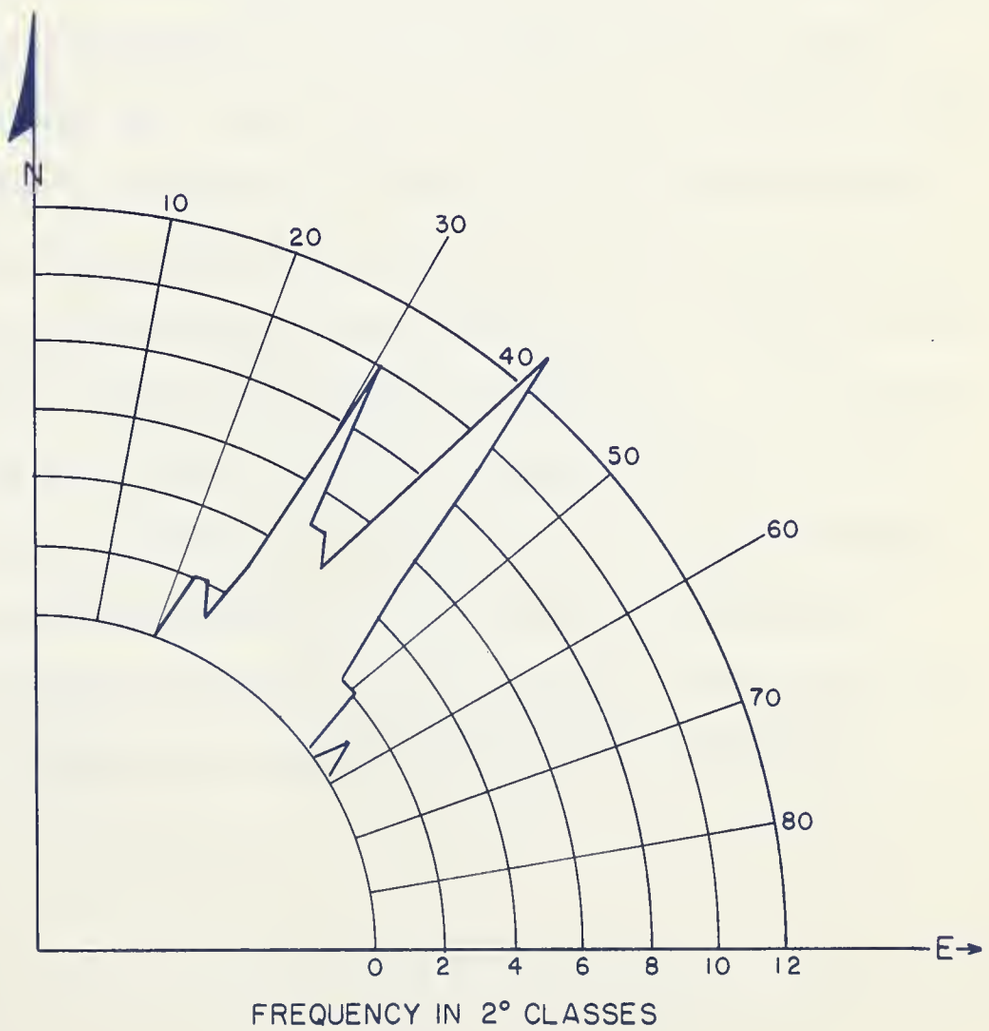


FIGURE 22

cleavage (Figure 10 b). The origin of the set is probably linked with late-stage elongation parallel to fold-axes (see Billings, 1954, pp. 117-8). Since the joints of set 1 are nearly perpendicular to fold-axes, they could not have been rotated appreciably by later folding, so that their present orientation relative to fold-axes approximately coincides with their orientation at the time of formation.

Set 2 also formed approximately perpendicular to bedding and its strike closely parallels the structural trend. The set is well developed in siltstones, but does not extend into adjacent argillites. The surfaces are rough and joints are often filled with 1/2 inch to 8 inches of vein-material, and in places with argillaceous material that has flowed in from adjacent argillites (Plate III b, c, and d). The trace of this set on set 1 can be seen in sub-area C, where it formed in tightly flexed siltstone beds (Plate II b). Since the set is in places displaced by set 3, and terminates sets 1, 5, and 6; it probably formed during the early stages of folding, a conclusion which is supported by the relation of its attitude to bedding and its absence from cleaved strata. The set may have originated as tensional fractures perpendicular to bedding. Its apparent restriction to the axial regions and to the northeastern limbs of anti-clines may be a consequence of the development of local tension in these regions, tension stemming from flexing in the case of fold-axes and extension during folding in the case of the steep limbs (see p. 41). On the other hand the joints of set 2 may have originated as fracture-

cleavage. Subsequent movement perpendicular to the fractures may have taken place later in the history of folding with the establishment of local tension in the fold-axes and steep limbs. The orientation of this joint-set with bedding horizontal is probably of greatest significance (Figure 23).

The restriction of sets 3 and 4 to sub-areas A and D may be either of genetic significance or because exposures in these areas make their recognition easier. Both sets have smooth faces and little or no vein-filling. Slickensides, with a bearing of north 50 degrees west and a plunge of about 20 degrees southeast, are abundant on set 3. The movement on this dominant set has been of the order of several feet in some cases, whereas the greatest observed displacement on set 4, on which slickensides were not observed, is only a fraction of an inch. Since sets 3 and 4 displace one another, and set 3 displaces set 2, it is concluded that sets 3 and 4 are contemporaneous shear-joints, which formed later than set 2 in response to an anomalous stress field in the anticlinal zones at some stage in the fold history. The acute bisectrix of the sets, which are at an angle of 45 degrees to one another, is approximately parallel to the fold-axes. Thus the maximum principal stress-axis at the time of formation of the joints appears to have been parallel to the fold-axes and the intermediate principal stress approximately perpendicular to bedding; a conclusion supported by the orientation of slickensides. Since joints similar to sets 2, 3, and 4 have been observed in gently folded strata (de Sitter, 1956, pp. 124-5), sets 3 and 4 probably formed early, soon after set 2,

FIGURE 23. Orientation of joints before and after rotation of bedding to the horizontal. The apparent grouping of sets 2, 3, and 4 in their field orientation is due to the better exposure on vertical limbs of folds. These joints can be seen in other orientations, but are difficult to measure (see Plate II b).

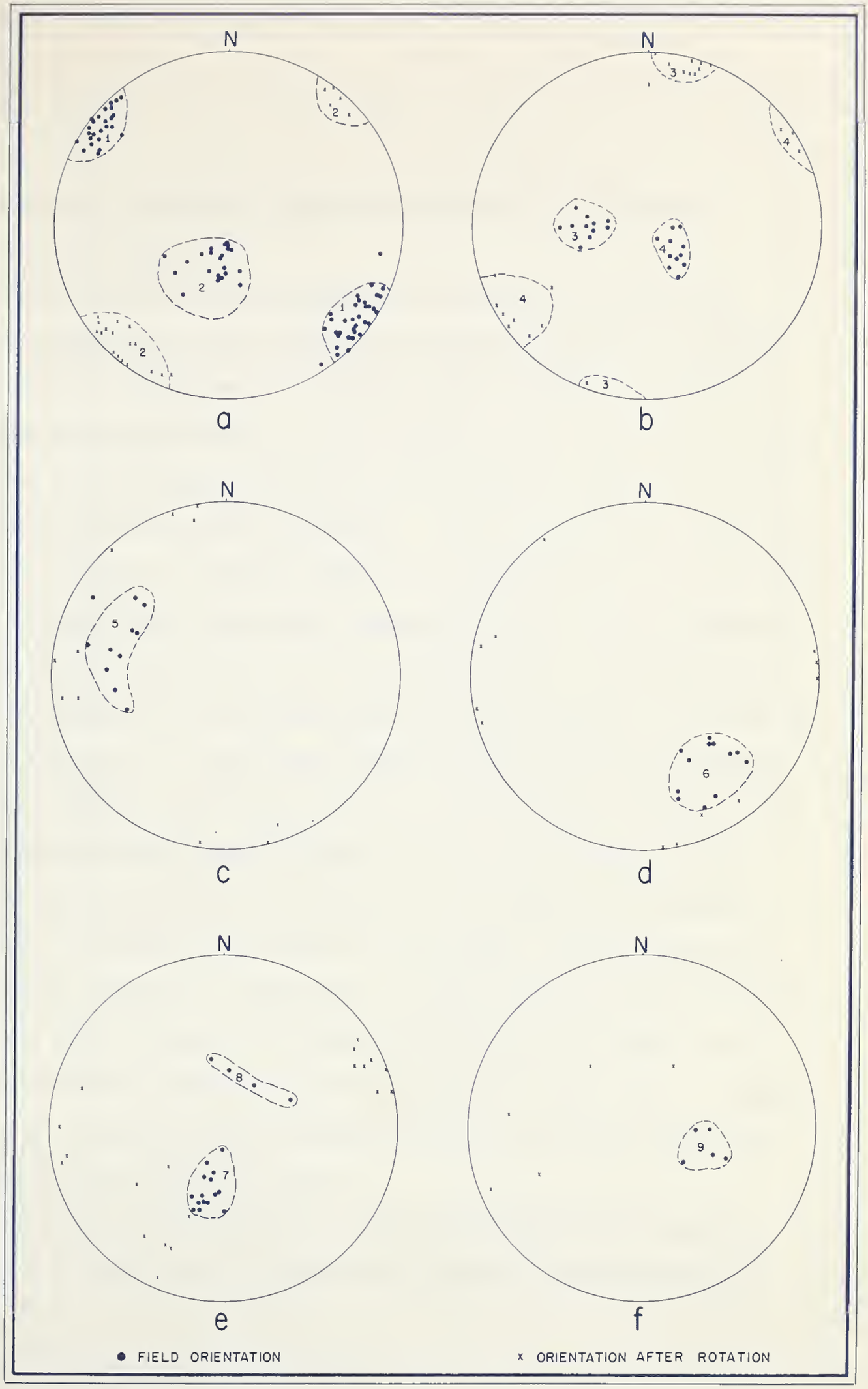
N
1
2
2
2
1
2
a
N
3
4
3
4
4
3
b
N
5
c
N
6
d
N
8
7
e
N
9
f
● FIELD ORIENTATION
x ORIENTATION AFTER ROTATION

FIGURE 23

so that their orientation with bedding horizontal is of genetic significance (Figure 23).

Sets 5 and 6 are poorly developed in the steeply dipping siltstones within the map-area, but are not found in argillites. They are approximately perpendicular to bedding, making an angle of roughly 70 degrees with one another, the acute bisectrix being slightly off vertical. Neither set is veined, and both tend to terminate at sets 1, 2, 3, and 4, indicating a later period of formation. The large variation in the orientation of these sets probably reflects the complicated nature of the local stress-fields within the steeply dipping and highly fractured siltstones which carried the weight of the overlying sediments. The influence of earlier joints on the position and size of these fractures can be seen in Plate III e and f. These joints probably represent post-stress-release shears, formed in response to a nearly vertical maximum principal stress.

The smooth and unveined joints of sets 7 and 8, which cut and in places displace argillite and siltstone in all areas, are independent of bedding, indicating a late period of development. The few observed displacements (Plate III g and h) seem to suggest that the joints are complementary shears, formed after folding but before stress-release. Set 9 is very similar in distribution and appearance to sets 7 and 8. Although its mode of origin is not immediately apparent, it probably formed late in the history of tectonic events.

The interpreted orientation of the stress field at the time of formation of each joint-set (Figure 19) indicates a northward migration

PLATE III

a. Looking up at a vertical cliff-face formed by a joint of set 1 in member B beds of sub-area C. Bedding is nearly horizontal. Note the intersecting planes of the same joint-set in the lower part of the photograph.

b. Trace of joint-set 2 on a cliff-face formed by joint-set 1. The former is present only in the siltstone beds.

c. Joint-set 2 in the upper siltstones of member A exposed along the Athabasca River. The large openings, now filled with vein material, probably reflect a discontinuous extension of the beds, the beginning of boudinage.

d. Large fracture of joint-set 2, filled with quartz, calcite, chlorite, and debris from the surrounding rock. Location is the same as above.

e & f. Field relationship of joint-sets 1 to 6, in the upper siltstones of member A near the Athabasca River. Note the control of the other sets on the position of sets 5 and 6.

g. Displacement on joint-set 7, cutting a small limestone bed as well as the surrounding argillite. Note the slump-structure in the limestone bed.

h. Displacement along a joint of set 8 in sub-area C. Bedding is approximately horizontal, cleavage dips 80 degrees southwest.

a


b


c

d

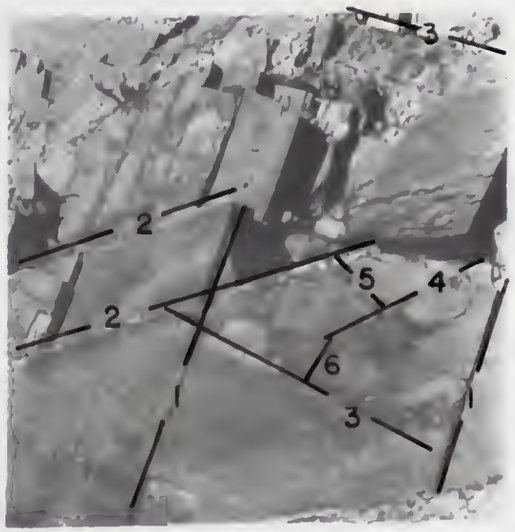


e


f


g

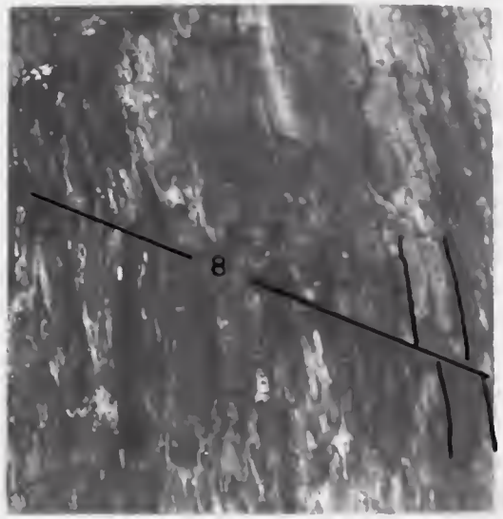


h

PLATE III


a. Looking up at a vertical cliff-face formed by a joint of set 1 in member B beds of sub-area C. Bedding is nearly horizontal. Note the intersecting planes of the same joint-set in the lower part of the photograph.

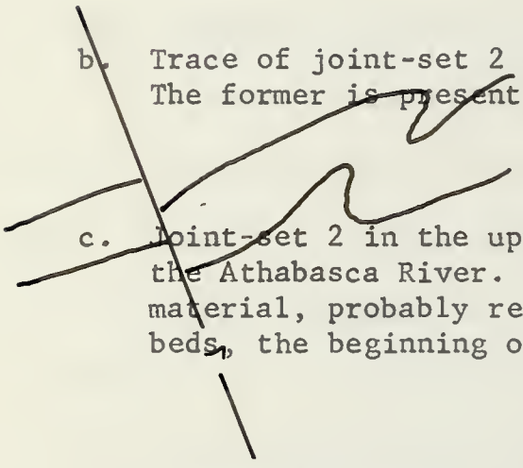


b. Trace of joint-set 2 on a cliff-face formed by joint-set 1. The former is present only in the siltstone beds.

c. Joint-set 2 in the upper siltstones of member A exposed along the Athabasca River. The large openings, now filled with vein material, probably reflect a discontinuous extension of the beds, the beginning of boudinage.

d. Large fracture of joint-set 2, filled with quartz, calcite, chlorite, and debris from the surrounding rock. Location is the same as above.

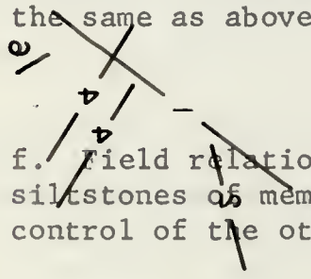


e & f. Field relationship of joint-sets 1 to 6, in the upper siltstones of member A near the Athabasca River. Note the control of the other sets on the position of sets 5 and 6.

g. Displacement on joint-set 7, cutting a small limestone bed as well as the surrounding argillite. Note the slump-structure in the limestone bed.

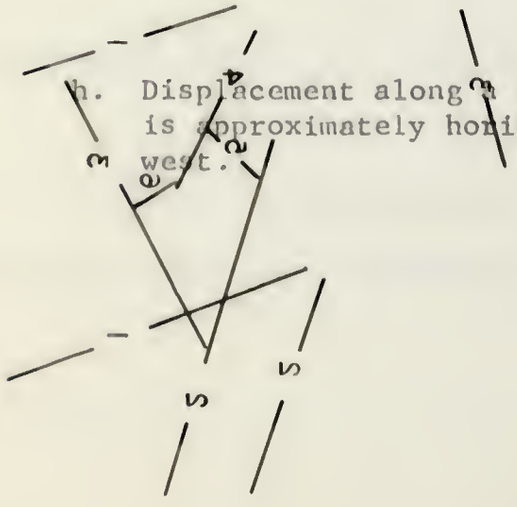


h. Displacement along a joint of set 8 in sub-area C. Bedding is approximately horizontal, cleavage dips 80 degrees southwest.

a

b

c

d

e

f

g

h

of the maximum principal stress-axis for younger joint sets. This may be related to the 22 degree difference in structural trend of the two parts of the Jasper anticlinorium (see p. 26). If this is the case, the joint analysis seems to indicate that the part of the anticlinorium southeast of the river was rotated clockwise about a vertical axis after the initiation of folding, but before stress-release. This rotation, or warping of axial planes may be connected with movement along the underlying Pyramid thrust-fault.

Summary of Tectonic Events. The following is an attempt to place the observed structural features of the Jasper anticlinorium in a logical sequence of tectonic events.

1. Initiation of folding.
2. Joints 1? 2, 3, and 4 formed in siltstone beds.
3. Fracture cleavage developed in siltstone beds, and flow cleavage in argillites.
4. Boudinage developed in steeply dipping siltstone beds.
5. Termination of folding and flow-cleavage.
6. Joint set 1 developed in argillites.
7. Warping of axial planes with re-orientation of previously formed lineations and foliations.
8. Termination of movement on the Pyramid thrust-fault.
9. Joint sets 7, 8, and possibly 9 formed.

10. Regional stress-release followed by development of joint-sets 5 and 6 in siltstone beds.

Since little or no evidence was found to indicate two periods of deformation, the tectonics of the area are attributed to the Laramide orogeny. However, the time spanning these features is unknown.

# METAMORPHISM

Introduction. The Old Fort Point strata of the Jasper anticlinorium fall within the quartz-albite-muscovite-chlorite subfacies of the greenschist facies (see Turner and Verhoogen, 1960, pp. 534 ff.). Although deformation of the area was almost certainly Laramide, preliminary potassium-argon age-dates indicate the possibility of a Palaeozoic period of metamorphism.

Characteristic Minerals.

Chlorite. As mentioned above, chlorite is present both as minute flakes and in books interleaved with muscovite (Plate IV a). An X-ray diffraction method developed by Shirozu (1958, pp. 209 ff.) was used to determine the composition of the chlorite in member C. The (060) and (0012) reflections were used to find the (010) and (001) d-spacings respectively. These values were found to be 9.22 A and 14.15 A, respectively, giving a composition for this chlorite as $(Fe, Mn)_{0.45}$ $(Mg)_{4.17}$ $(Fe,Al)_{1.38}(Al_{1.38}Si_{2.62})$ $O_{10}$ $(OH)_8$.

The X-ray determination was supplemented by an optical determination outlined by Hey (1954, p. 277). The mineral was found to be optically negative with a birefringence of about 0.010, and $N_w$ of 1.59. When this data is plotted on Hey's diagram, the following results are obtained:

Fe Total / Fe + Mg = 0.67

Total Fe = 2.61

Total Si = 4.00

These values, calculated on the basis of 14 oxygen atoms, may be compared with the X-ray values by recalculating the latter on the same basis. The X-ray values, when recalculated on the basis of 14 oxygen atoms, give a silicon value of 3.67 as compared with 4.00 obtained optically, indicating a discrepancy of only about 8 per cent. By combining the two methods, it was found that only 25 per cent of the total iron present was in the ferrous state, thus placing the chlorite in the delessite field.

Muscovite. An attempt was made to identify the muscovite present in the argillite of member C, using an X-ray diffraction method developed by Yoder and Eugster (1955, p. 225). Although certain difficulties, arising from the presence of other minerals in the sample, were encountered, the results strongly suggest a muscovite of the 2M variety.

The origin of the chlorite-muscovite books is not understood. In cleaved argillites, the elliptical books tend to lie with their long axes in the cleavage plane parallel to the a tectonic direction. Since the c axes of the chlorite and muscovite flakes which make up the books tend to coincide with the longest axis of the grain, these flakes tend to be perpendicular to cleavage, even where the latter is parallel to bedding (Plate IV g). In the uncleaved siltstones, the books are tabular, with the c axes of the component minerals perpendicular to bedding, coinciding with the shortest dimension of the grain. A possible explanation may be

that original detrital grains, possibly biotite, expanded along their c crystallographic axes prior to the initiation of cleavage in the argillites. This expansion was probably accompanied by conversion to chlorite and muscovite, the more stable minerals at the prevailing conditions of temperature and pressure. When folding occurred and cleavage developed, the chlorite-muscovite books acted as discrete grains, despite the micaceous nature of their components. The long axis of each grain apparently rotated into the cleavage plane, became parallel to the a tectonic direction, and maintained this orientation throughout the remainder of the fold history. Since the controlling factor in the orientation of the chlorite and muscovite in the books is the overall shape of the books, rather than the crystallographic orientation of the components, the cleavage exhibited by these argillites may be due largely to mechanical re-orientation of platy minerals. Although recrystallization may have played a greater role in the re-orientation of finer-grained material, the small amount of argon loss during Laramide deformation (see p. 81) suggests that this also was largely mechanical.

Quartz. Numerous delicate overgrowths of quartz are present in the quartzose limestone-breccia of member C, confirming its stability in this environment (Plate IV b).

Albite. Albite is an important constituent of this suite of rocks. Its formation by albitization of calcic and potassic feldspar has apparently been augmented by authigenic growth (Plate IV c). The grain in the photomicrograph appears to be albitized plagioclase with an overgrowth of authigenic albite. The numerous calcite inclusions in the centre of the grain

suggest the breakdown of calcic plagioclase to give albite and calcite. Growth of this mineral seems to have occurred preferentially in the limestones of member B, where albite is 1.5 times as abundant as quartz. Refractive indices of $n_z = 1.538$ and $n_y = 1.532$ indicate albite of $An_o$ composition, using the curves presented by Smith (1958, p. 1189).

Calcite. Calcite rather than epidote appears to be the stable calcic phase. The alteration of calcic plagioclase to albite and calcite mentioned above, as well as numerous instances of calcite recrystallization and twinning seem to support this conclusion. The limestone phenoclasts of member B breccias often exhibit recrystallized boundaries in which quartz and albite grains have been excluded outwards to the boundary with the breccia matrix (Plate IV d). The stability of the calcite phase seems to indicate a high partial pressure of carbon dioxide during metamorphism.

Biotite. Biotite flakes were observed in the fine-grained sands of member D. Biotite appears to be unstable at this low grade of regional metamorphism, altering to books of chlorite and muscovite, so that its presence is probably a function of the slow rate of this reaction.

Siderite. It is difficult to determine whether or not the minute siderite rhombs were stable during metamorphism.

Heavy minerals. Detrital grains of zircon, tourmaline, and ilmenite are present, but show no evidence of authigenic growth.

Age of Metamorphism. The Canadian Rocky Mountains apparently underwent orogenesis in lower Tertiary times (Russell, 1954, p. 68). It would therefore appear reasonable to conclude that the Precambrian strata of the Old Fort Point formation were metamorphosed at this time. In order to ascertain the validity of this conclusion, and at the same time test the potassium-argon whole-rock method on low-grade metamorphics, three age dates were obtained from the argillite of member C. Sample 1 (AK 182) was collected from poorly cleaved strata near the type locality of member D, sample 2 (AK 187) from well cleaved argillite of section 18 (Figure 2), and sample 3 (AK 184) from phyllite of the same horizon, collected in a railroad cut 1/2 mile west of Giekie (10 miles west of Old Fort Point). The increasing development of cleavage from east to west can be seen from Plate IV e, f, and g. The dates obtained were 346, 333, and 286 million years for samples 1, 2, and 3, respectively, with a maximum analytical error of plus or minus 15 million years.

Since the basic assumption as to the age of metamorphism is not reflected in the dates obtained, little can be said about the validity of the method as applied to these rocks, and the project must be regarded as a failure. However, it is perhaps worthwhile to speculate on the meaning of these results. While a few possibilities are listed below, others undoubtedly exist.

It is possible that these dates reflect an age intermediate between the age of the detrital material coming from the Canadian Shield, and that of the lower Tertiary Laramide orogeny. The decreasing ages obtained

PLATE IV

a. Chlorite-muscovite book from a breccia lens near section 13, (Figure 2). Crossed nicols, X 64.

b. Overgrowth on a quartz grain in the matrix of the quartzose limestone-breccia of member C. Dark rim is inclusions of calcite, marking the original boundary of the grain. Crossed nicols, X 25.

c. Albite grain from the matrix of the quartzose limestone-breccia of member C. Dark interior contains calcite inclusions, while the light outer rim of apparently authigenic albite contains relatively few calcite inclusions. Crossed nicols, X 32.

d. Recrystallized boundary of a limestone phenoclast from the base of the thick breccia unit at Old Fort Point. Note the apparent exclusion of quartz and albite grains from the recrystallized calcite. Crossed nicols, X 32.

e. Poorly cleaved argillite from member C from which a date of 346 million years was obtained. Dark streak in lower left corner is a chlorite vein. Sample was collected from the top of member C near the type locality of member D (Figure 2). Crossed nicols, X 25.

f. Well cleaved argillite from member C at section 18 (Figure 2). The sample gave a date of 333 million years. Note the orientation of chlorite and muscovite flakes in the elliptical books. X 16.

g. Phyllite from member C, 10 miles to the west of Old Fort Point. Bedding and cleavage are nearly parallel, and chlorite and muscovite flakes in the elliptical book are perpendicular to cleavage. Sample gave a date of 286 million years. X 16.

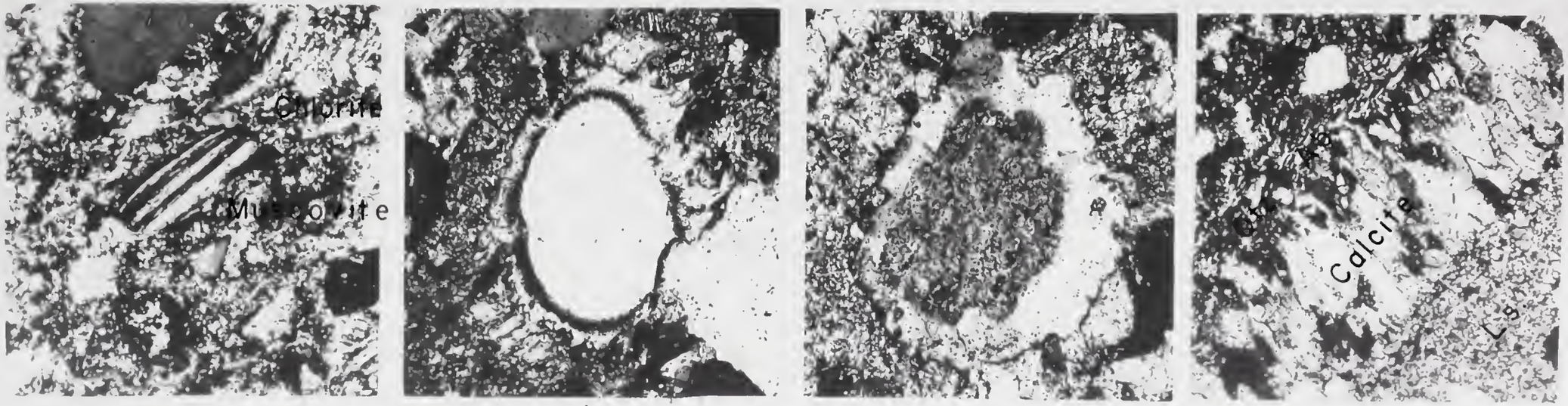


a b c d

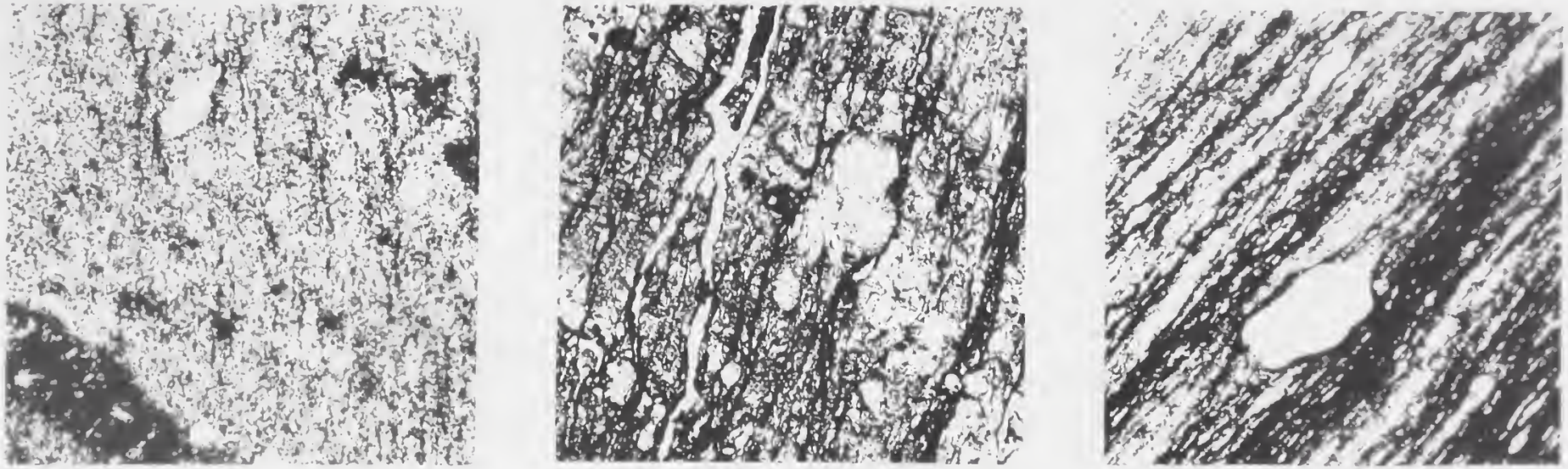

e f g

PLATE IV

a. Chlorite-muscovite book from a breccia lens near section 13, (Figure 2). Crossed nicols, X 64.

b. Overgrowth on a quartz grain in the matrix of the quartzose limestone-breccia of member C. Dark rim is inclusions of calcite, marking the original boundary of the grain. Crossed nicols, X 25.

c. Albite grain from the matrix of the quartzose limestone-breccia of member C. Dark interior contains calcite inclusions, while the light outer rim of apparently authigenic albite contains relatively few calcite inclusions. Crossed nicols, X 32.

d. Recrystallized boundary of a limestone phenoclast from the base of the thick breccia unit at Old Fort Point. Note the apparent exclusion of quartz and albite grains from the recrystallized calcite. Crossed nicols, X 32.

e. Poorly cleaved argillite from member C from which a date of 346 million years was obtained. Dark streak in lower left corner is a chlorite vein. Sample was collected from the top of member C near the type locality of member D (Figure 2). Crossed nicols, X 25.

f. Well cleaved argillite from member C at section 18 (Figure 2). The sample gave a date of 333 million years. Note the orientation of chlorite and muscovite flakes in the elliptical books. X 16.

g. Phyllite from member C, 10 miles to the west of Old Fort Point. Bedding and cleavage are nearly parallel, and chlorite and muscovite flakes in the elliptical book are perpendicular to cleavage. Sample gave a date of 286 million years. X 16.

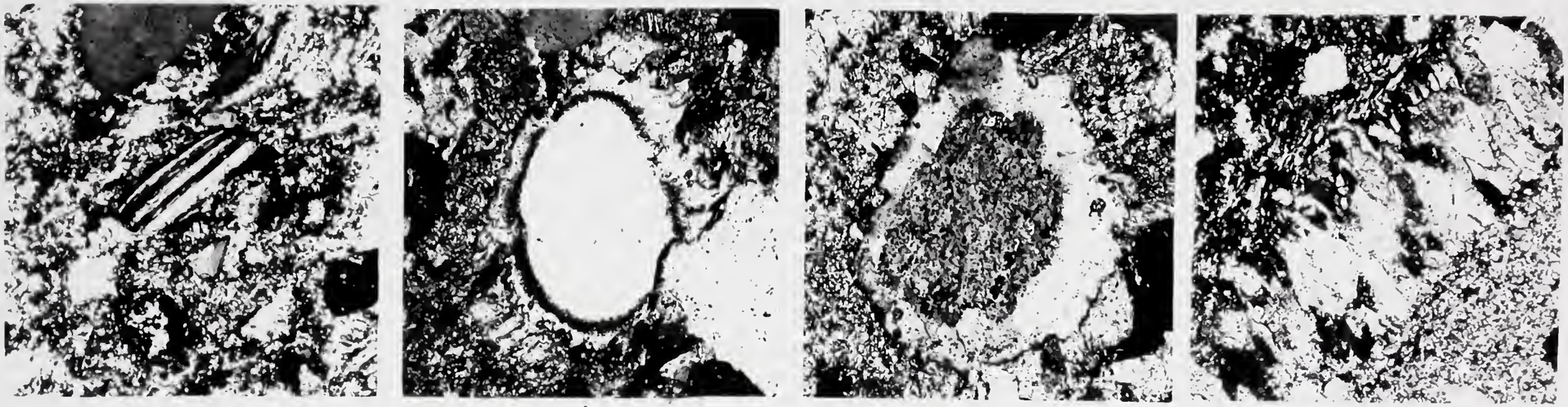
a
b
c
d


e
f
g

from argillites of increasing intensity of dynamic metamorphism are in agreement with this conclusion.

A second possibility is that an increase in the geothermal gradient in Devonian time may have led to the crystallization of chlorite and muscovite and complete loss of argon from detrital material. On this basis, the present Carboniferous dates are a reflection of updating during the Laramide orogeny. The relatively small amount of argon loss possibly indicates that little recrystallization took place during this orogeny. The Devonian thermal metamorphism may have occurred contemporaneously with the intrusion of the Ice River complex and with the period of epeirogenesis related to the pre-Upper Devonian unconformity (Harker, Hutchinson, and McLaren, 1954, p. 48 ff.). If this is the case, one might expect to find evidence of two orogenies some distance to the west of the map-area.

A third possibility is that the rocks of the main ranges were folded during a Palaeozoic orogeny, and underwent little or no deformation other than thrust-faulting during the later Laramide orogeny. At present, there appears to be little stratigraphic evidence to support this conclusion.

## REFERENCES CITED

Billings, M.P., 1954, Structural geology, 2nd Ed.: Prentice-Hall, Englewood Cliffs, N.J.

Charlesworth, H.A.K. and Remington, D.B., 1960, Precambrian rocks in the vicinity of Jasper, Alberta: Edm. Geol. Soc., 2nd Annual Field Conference, Guide Book, p. 13.

Cloos, E., 1947, Oolite deformation in the south mountain fold, Maryland: Bull. Geol. Soc. Amer., vol. 58, no. 9, pp. 843-915.

Harker, P., Hutchinson, R.D., and McLaren, D.J., 1954, The sub-Devonian unconformity in the eastern Rocky Mountains of Canada: Western Canada Sedimentary Basin, Amer. Assoc. Petrol. Geol. Symposium, Rutherford Memorial Volume, pp. 48-66.

Hey, M.H., 1954, A new review of chlorites: Min. Mag., vol. 30, pp. 224.

Kuenen, Ph. H., and Migliorine, C.I., 1950, Turbidity currents as a cause of graded bedding: Jour. Geol., vol. 58, pp. 91-127.

Remington, D.B., 1960, Precambrian rocks of the Whistlers Mountain trail map-area, Jasper: unpublished Master's thesis, p. 23.

Rich, J.L., 1951, Three critical environments of deposition and criteria for recognition of rocks deposited in each of them: Bull. Geol. Soc. Amer., vol. 62, pp. 1-20.

Russell, L.S., 1954, The Eocene-Oligocene transition as a time of major orogeny in western North America: Trans. Roy. Soc. Can., vol. 48, sec. 4, series 3, pp. 65-9.

Sander, B., 1930, Gefugekunde der Gesteine: Julius Springer, Wien, p. 119.

Shirozu, H., 1958, X-ray powder patterns and cell dimensions of some chlorites in Japan, with a note on their interference colors: Min. Jour., vol. 2, no. 4, pp. 209-33.

Sitter, L.U. de, 1956, Structural geology: McGraw-Hill, New York.

------, 1958, Boudins and parasitic folds in relation to cleavage and folding: Geologie en Mijnbouw, N. W. Ser., 20e, Nummer 8, pp. 277-86.

Smith, J.R., 1958, The optical properties of heated plagioclases: Amer. Min., vol. 43, pp. 1179-94.

Sutherland-Brown, A., 1957, Geology of the Antler Creek area, Cariboo District, British Columbia: British Columbia Dept. Mines Bull. 38.

Turner, F.J. and Verhoogen, J., 1960, Igneous and metamorphic petrology, 2nd Ed: McGraw-Hill, New York.

Walcott, C.D., 1910, Pre-Cambrian rocks of the Bow River Valley, Alberta, Canada: Smithsonian Misc. Coll., vol. 53, no. 7, pp. 423-31.

Yoder, H.S., and Eugster, H.P., Synthetic and natural muscovites: Geochim. et Cosmochim. Acta, vol. 8, pp. 225-80.